



## Research Article

## Secondary metabolite profiling using HR-LCMS, antioxidant and anticancer activity of *Bacillus cereus* PSMS6 methanolic extract: *In silico* and *in vitro* study

Shalini TS<sup>a</sup>, Manivel G<sup>a</sup>, Krishna kumar G<sup>a</sup>, Prathiviraj Ragothaman<sup>b</sup>, Rajesh Kannan Velu<sup>c</sup>, Senthilraja P<sup>a,\*</sup>

<sup>a</sup> Department of Bioinformatics, Bharathidasan University, Tiruchirappalli, Tamil Nadu, 620 024, India

<sup>b</sup> Department of Microbiology, School of Life Sciences, Pondicherry University, Puducherry 605014, India

<sup>c</sup> Department of Microbiology, Bharathidasan University, Tiruchirappalli, Tamil Nadu, 620 024, India

## ARTICLE INFO

## Keywords:

HRLC-MS  
HER2  
Antioxidant  
MTT assay  
*Bacillus cereus*  
Molecular docking

## ABSTRACT

Novel anticancer drugs of natural origin have increased tremendously due to the resistance of multiple chemotherapeutic drugs in breast cancer therapy and their high toxicity with undesirable side effects. The study investigates the bioactivity of secondary metabolites derived from *Bacillus cereus* PSMS6 isolated from marine soil sediment in the Velar estuary, Parangepattai, Cuddalore district, Tamil Nadu, and India. Strains were isolated and antagonistic activity was screened using the agar well diffusion method. *B. cereus* PSMS6 exhibited potency, and its crude extract was tested for antioxidant, anticancer, and cytotoxic MTT assay potential. The methanolic extract of *B. cereus* PSMS6 was analyzed by mass spectrometry HRLC-MS and FT-IR to determine the bioactive compounds. A drug interaction study with the anti-breast cancer protein HER2 was performed by molecular docking analysis. Antioxidant activities were determined using total antioxidant scavenging assay, ABTS and DPPH free radical scavenging assays. The total antioxidant scavenging assay of the crude extract of *B. cereus* methanol had an IC<sub>50</sub> value of 28.33±1.01, in ABTS IC<sub>50</sub> value of the extract was 29.00±0.28 and in DPPH the IC<sub>50</sub> of the extract was 34.91±0.09. The negative ion compound Palmitoylglycerone phosphate had a LibDock score of 149.487 and the positive ion compound N5-(4-Methoxybenzyl) glutamine had 120.116. These compounds show promising anticancer activity. The current study reported that the bioactive secondary metabolite of *B. cereus* PSMS6 retains anti-cancer, and antioxidant properties. This is the first report to show the production of the Palmitoylglycerone phosphate metabolite from *B. cereus* PSMS6.

## Abbreviations

ABTS	2,2'-Azino-bis(3-ethylbenzthiazoline-6-sulfonic acid)
BLAST	Basic Local Alignment Search Tool
DMEM	Dulbecco's modified Eagle Medium
DPPH	2,2-diphenyl-1-picrylhydrazyl
EGF	Epidermal growth factor
EGFR	Epidermal growth factor receptor
FBS	Fetal Bovine Serum
FT-IR	Fourier Transform – Infrared
HER2	Human epidermal growth factor receptor 2
HPLC	High-performance liquid chromatography
HR	Hormone Receptor

HR-LCMS	High-Resolution Liquid Chromatograph Mass Spectrometry Analysis
IC <sub>50</sub>	Inhibitory Concentration
CC <sub>50</sub>	Cytotoxic Concentration
TI	Therapeutic Index
ITS1	Internal Transcribed Spacers 1
ITS2	Internal Transcribed Spacers 2
MEGA	Molecular Evolutionary Genetics Analysis
NCBI	National Centre for Biotechnology Information
NCCS	National Centre for Cell Science
PDB	Protein Data Bank
PPINs	Protein-protein interaction networks
rDNA	Ribosomal DNA

\* Corresponding author.

E-mail address: [senthilraja.p@bdu.ac.in](mailto:senthilraja.p@bdu.ac.in) (S. P).

<https://doi.org/10.1016/j.btr.2024.e00842>

Received 12 February 2024; Received in revised form 24 April 2024; Accepted 25 April 2024

Available online 2 May 2024

2215-017X/© 2024 The Author(s). Published by Elsevier B.V. This is an open access article under the CC BY-NC license (<http://creativecommons.org/licenses/by-nc/4.0/>).

TGF- $\alpha$  Transforming growth factor alpha

## 1. Introduction

Breast cancer is the leading cause of cancer mortality in women worldwide. Understanding and treating breast cancer on a worldwide basis depends heavily on epidemiology. The disease is correlated with human development, but survival rates are less favourable in less developed regions. The rate of incidence is significantly higher among old-aged women and the median age of breast cancer diagnosis was 63 years from year 2014–2018, which has increased to 69 years during the years 2015–2019. However, the mortality rate has been reduced by 1.1 % during 2013–2019 [1]. The World Health Organization (WHO) launched the Global Breast Cancer Initiative to improve survival rates through health promotion, timely diagnosis, comprehensive treatment, and supportive care [2]. Breast cancer was a contributing factor in over 6,85,000 female deaths globally in 2020. Also, 3,00,590 new cases and 43,700 deaths of breast cancer in the United States, were reported in 2023 [3]. Nearly two-thirds of the fatalities were recorded in less-developed areas. From the last 5-year survival rate for breast cancer is much over 80 % in more developed countries. More than 50 % of South Africans and less than 70 % of Indians, respectively, are thought to have died within five years [4].

The global age-standardized breast cancer incidence rate is 48/100,000, with varying rates in sub-Saharan Africa, Western Europe, and North America. Age is the maximum essential hazard factor, with the very best occurrence rates located inside the oldest females [5]. Almost 70 % of BC have a positive hormone receptor (HR) and a positive human epidermal growth factor receptor 2 (HER2) [6]. Epidermal growth factor receptor (EGFR) is a cellular receptor that performs a crucial characteristic in cellular growth, proliferation, and survival. It is a member of the *ErbB* family of receptors and is activated through interacting with certain ligands, such as epidermal growth factor (EGF) and transforming growth factor alpha (TGF- $\alpha$ ). Once activated, EGFR triggers a signalling cascade that leads to various cellular responses, including DNA synthesis, cell division, and migration [7]. The *ERBB2* gene encodes for HER2 which is located on chromosome 17 and plays a crucial role in cell growth and division in *Homo sapiens* [8]. Overexpression or amplification of the HER2 protein is associated with aggressive forms of breast cancer, making it an important target for therapeutic interventions. Overexpression of HER2, EGFR, and other receptor tyrosine kinases plays a major role in breast cancer [9]. This HER2 is an oncogene, a receptor tyrosine kinase that promotes cell growth and survival. Targeted therapies such as Trastuzumab have been developed to specifically inhibit the activity of HER2 and improve the outcomes for individuals who have HER2-positive breast cancer [10].

New therapies are being investigated in breast cancer, such as gene therapy, breast cancer vaccines, adoptive cell therapies, including T cell receptor therapy etc. Most of them are still ongoing [3]. Drug agents, such as Trastuzumab and Pertuzumab, have shown remarkable efficacy in inhibiting the growth of HER2-positive tumours. They work by specifically targeting the HER2 receptor, blocking this signalling pathway and preventing cancer cell proliferation [11]. Microbial communities play a vital role in nutrient cycling, carbon sequestration, and the breakdown of organic matter in marine sediments. Additionally, they contribute to the overall health and stability of marine ecosystems by regulating water quality and supporting the growth of other organisms through symbiotic relationships [12]. Ribosomal DNA (rDNA), is a phylogenetic marker that is frequently employed in taxonomy research and phylogenetic inferences. Prokaryotic rDNA has three subunits (5S, 16S, and 23S) which differentiate them from eukaryotes, together with two internal transcribed spacers (ITS1 and ITS2) that have various rates of evolution [13]. Each site can be evaluated separately for phylogenetic purposes, and the choice of a certain location depends on the taxonomic level. So, for phylogenetic inferences of closely related species or genera, areas with fast evolution are considered. Numerous methods are

available to construct phylogenetic trees that predict the relatedness between microbial species. In our study, we collected the marine soil sample and characterized the microorganisms using 16S rDNA sequencing. From the sequencing data, the microbial species were classified into clades after analyzing the complete dataset with neighbor-joining and a basic heuristic search based on maximum parsimony [14]. The associated taxa are clustered together in the bootstrap method with 1000 replicates. Various compounds from both marine and freshwater organisms can be isolated using efficient techniques like high-performance liquid chromatography (HPLC) [15]. Of all the microbes isolated, *B. cereus* was chosen for the identification of secondary metabolites using HPLC-MS from the crude extract. The species was confirmed based on the 16S rRNA gene and morphological characterization based on its biological activity. The antioxidant capability of the *B. cereus* methanolic crude extract was determined using various free radical scavenging assays.

Breast cancer treatment faces unmet needs, including improving efficacy, minimizing adverse effects, and reducing cancer recurrence. Current therapies, such as chemotherapy and radiation, struggle with drug resistance and incomplete eradication. The antioxidant capability of *B. cereus* methanolic crude extract could address these issues by scavenging free radicals and reducing oxidative stress. This could enhance conventional cancer therapies, target drug-resistant tumors, and prevent cancer recurrence, offering novel therapeutic options that can improve patient outcomes. A molecular docking study has been performed on the secondary metabolites derived from the crude extract in relation to the target protein. We have chosen to restrict the compounds included in the docking study to those whose structures have been adequately defined to allow for obvious identification and matching with available data. Furthermore, *in silico* studies use computer-based models to find and filter certain extract components that have strong anti-breast cancer capabilities. The study focuses on the effectiveness of the bacterial crude extract in inhibiting the proliferation and cell division of MCF-7 breast cancer cells. Also, we performed a cytotoxicity assay to validate our findings.

## 2. Materials and methods

### 2.1. Sample collection

The samples were obtained from the marine soil sediments of the Velar estuary, Parangipettai, Tamil Nadu, India (Latitude. 11°29'24.9"N and Longitude. 79°45'56.6"E). Bacterial isolation was carried out by serial dilution of samples, 1 g of soil dissolved in 9 ml of distilled water. The samples were serially diluted and dilutions (dilutions taken for the experiment) it was spread-plated on Luria Bertani (LB) (pH of the medium) agar plates. Plates were incubated at 37°C for 24 hrs. The isolated colonies were further cultured by quadrant streaking method to obtain pure culture and were maintained in a nutrient agar slant.

### 2.2. DNA extraction

Bacterial culture was taken (2 ml) and centrifuged at 8000 rpm for 15 min. The supernatant was discarded, and the pellet was collected and resuspended in 500  $\mu$ l of Solution - I (10 mm Tris, 10 mm MgCl<sub>2</sub>, 20 mm EDTA, 40 mm NaCl, 10 mm KCl) and 50  $\mu$ l of Lysozyme. The sample was vortexed and incubated at 37°C for 1 h. 20 % of SDS (30  $\mu$ l) was added along with 5  $\mu$ l of proteinase K and incubated at 65°C for 30 min and cooled. 40  $\mu$ l of 5 M NaCl and 32  $\mu$ l of CTAB/NaCl were added and incubated at 60°C for 10 min. Then an equal volume of freshly prepared Chloroform: Isoamyl alcohol (24:1) was added and the solution color turned into milky white. The solution was centrifuged at 8000 rpm for 10 min, the aqueous layer was separated into a new Eppendorf tube. 500  $\mu$ l of pre-chilled ethanol (% of ethanol used) was added and it was maintained at -20°C overnight. The solution was then centrifuged at 10,000 rpm for 15 min. The pellet was air-dried and reconstituted in 50

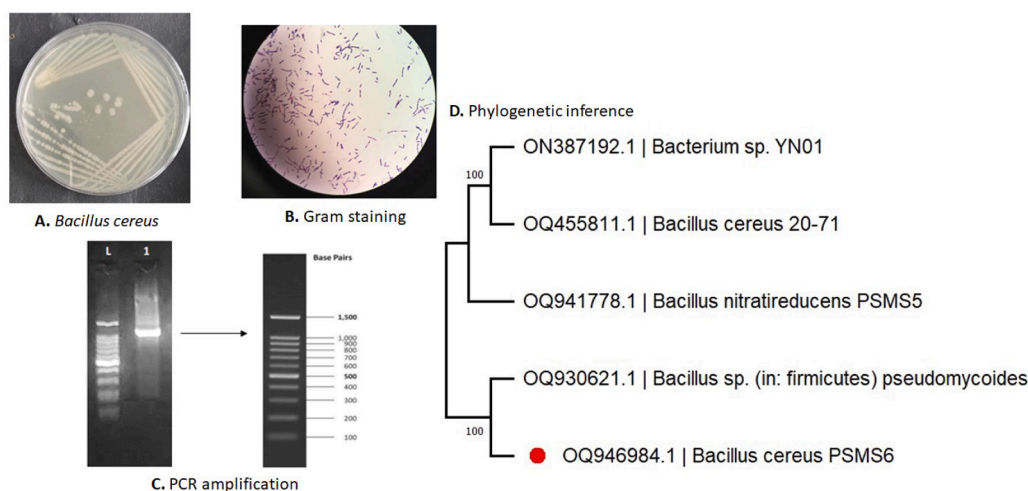


**Fig. 1.** Morphological characterization and identification of *B. cereus* by 16S rRNA gene sequencing. (A) *Bacillus cereus* culture plate, (B) microscopic view, (C) PCR amplification, and (D) Phylogenetic evaluation.

**Table 1**  
FT-IR analysis of *B. cereus* crude extract.

S. No.	Wavelength (cm <sup>-1</sup> )	Functional group	Compound class
1	3790.4	O-H stretching	Alcohol
2	3338.18	N-H stretching	Aliphatic primary amine
3	2401.91	O=C=O stretching	Carbon dioxide
4	2348.87	O=C=O stretching	Carbon dioxide
5	2078.89	N=C=S stretching	Isothiocyanate
6	1630.52	C=C stretching	Cyclic alkene
7	1530.24	N-O stretching	Nitro compound
8	1402.96	S=O stretching	Sulfonyl chloride
9	1273.75	C-O stretching	Aromatic ester
10	1222.65	C-O stretching	Vinyl ether

μl of TE buffer [16]. After this step, DNA was run in 0.8 % Agarose Gel electrophoresis 50X TAE buffer 6X Gel loading dye and Ethidium bromide solution. The PCR reaction mixture used had 5 μl of Master mix containing: 1 μl of Forward primer, 1 μl of Reverse primer, 1 μl DNA and 2 μl of MilliQ water. The PCR reaction was carried out by an initial denaturation step at 95°C for 3 mins followed by 35 cycles of denaturation at 94°C to 40 secs annealing temperature of 46°C for 45 s and elongation at 72°C for 15 min. Amplification of DNA was confirmed by 1.2 % agarose gel electrophoresis [17].

### 2.3. Phylogenetic analysis

The 16S rRNA gene of the marine strain was sequenced and the obtained result was matched with existing sequence data present in NCBI [18] using BLAST [19]. Phylogenetic analysis was carried out by using MEGA 11.0 software [20]. The evolutionary history was interpreted by using the Neighbor-Joining method [21]. The pairwise genetic diversity and Tajima's neutrality test [22] were computed among the selected phylogenetic neighbours.

### 2.4. Mass cultivation of bacteria

For mass cultivation, the bacterial strain *B. cereus* was grown in 50 ml of Luria Bertani broth (LB) and incubated at 37°C for 24 h. Then prepared seed culture was transferred into a 1000 ml mass culture medium incubated in a rotary shaker at 120 rpm at 37°C for five days.

### 2.5. Extraction of secondary metabolite and preparation of crude extract

Following the incubation time, the pellet was disposed of and the

bacterial culture was centrifuged for 20 min at 8000 rpm. Using a 0.22 μm membrane filter, the resulting supernatant was filtered as part of a purification process to eliminate bacterial organisms. After that, the cell-free supernatant was combined with an equivalent amount of ethyl acetate (1:1 v/v) and agitated for 24 h at 120 rpm. A solvent extraction funnel was used to isolate the ethyl acetate phase, which was then concentrated under a rotating vacuum evaporator. Following that, it was dried at 72°C with a magnetic stirrer. Then after, the crude extract was kept in storage at -20°C.

### 2.6. Fourier transform – infrared (FT-IR) analysis

*B. cereus* crude extracts were taken as dry powder. 1 mg of the crude extract was dissolved in 1 ml of distilled water. Utilizing FT-IR spectroscopy, the sample was placed in a sample holder and its spectrum was captured between 4600 and 450 cm<sup>-1</sup> range [23].

## 3. Antioxidant activity

### 3.1. Total antioxidant radical scavenging activity

The total antioxidant content of methanol extracts of *B. cereus* bacteria was estimated using a Folin-Ciocalteu reagent-based assay, using ascorbic acid as a standard [24]. The extract was dissolved in methanol, 500 μl of reagent, and 20 % Na<sub>2</sub>CO<sub>3</sub> added. The colour was recorded at 765 nm using a UV-vis spectrophotometer.

$$\% \text{ of total antioxidant} = \frac{\text{Concentration of Ascorbic acid}}{\text{Weight of extract}} \times \text{volume of extract}$$

### 3.2. ABTS scavenging activity

The ABTS radical cation decolourization assay measured the antioxidant activity of marine *B. cereus*. The method involved reacting 7 mM ABTS with 5 mM potassium persulfate for 12–16 h, then adding a diluted ABTS solution to the crude extract at varying concentrations. The absorbance was recorded (nm), and the percentage of inhibition was calculated [25].

$$\% \text{ Scavenging} = \frac{\text{Control OD} - \text{Test OD}}{\text{Control OD}} \times 100$$

### 3.3. DPPH radical scavenging activity

In order to transform into a stable diamagnetic molecule, DPPH, a

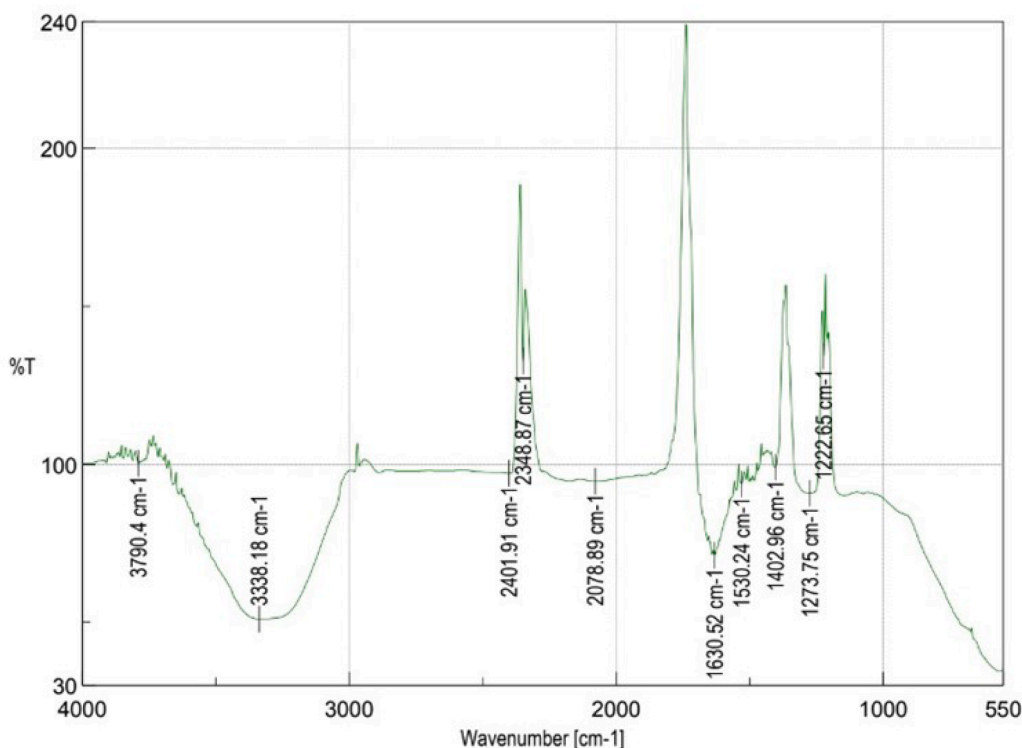


Fig. 2. FT-IR analysis of *B. cereus* crude extract.

stable free radical, must either accept an electron or a hydrogen radical. An antioxidant substance that can donate hydrogen and is reduced from reacting with DPPH. It was measured how the colour changed (from deep violet to pale yellow). The yellow colour intensity in a sample is directly linked to the concentration and effectiveness of radical scavengers. Higher antioxidant concentrations reduce DPPH radicals, while different types of scavengers affect colour intensity. The strength and composition of these scavengers determine DPPH radical scavenging activity. We collected sample extracts at various concentrations and adjusted the volume to the solvent. The extraction solutions of 0.1 mM DPPH were added to the various concentrations of the crude extract and vigorously vortexed at 900 rpm. The tubes were left to stand at 27 °C for 20 min. At 517 nm, the sample's absorbance was measured. The expression of radical scavenging activity was expressed as the sample extracts' efficiency in trying to prevent the formation of free radicals. The sample's capacity to scavenge free radicals increases with increasing inhibition percentage. The findings revealed a dose-dependent effect, with the inhibition percentage increasing as the concentration of the sample extracts did. Additionally, the level of radical scavenging activity varied between samples, indicating that the type of radical scavenger in each sample affected how much inhibition was present. It was determined by applying the formula: % of *B. cereus* extracts at various concentrations (125, 250, 500, and 1000 g/ml) were taken, 1 ml of DPPH was added, and this was made up to 3 ml with distilled water. 30 min at room temperature were given for the tubes to stand. A positive control was ascorbic acid. The changes in absorbance of the sample and control were measured in a spectrophotometer at 514 nm, and the experiment was carried out in triplicate. A control without extract was also prepared. Using the following formula, the percentage of DPPH decolorization in the samples was calculated [26].

$$\% \text{ Scavenging} = \frac{\text{Absorbance of control} - \text{Absorbance of sample}}{\text{Absorbance of Control}} \times 100$$

#### 3.4. High-Resolution liquid chromatograph mass spectrometry analysis

Using an Agilent 1200 LC system, the crude extract was subjected to an HR-LCMS analysis to profile *B. cereus* secondary metabolites. At the SAIF facility of the Indian Institute of Technology in Mumbai, India, the identification of *B. cereus* secondary metabolites by LC-MS analysis was done. Further analysis of the *B. cereus* crude extracts involved HRLC-MS using a G6550A quadrupole time-of-flight mass spectrometer and an ionization method lasting 30 min in ESI 10,032,014-positive mode. The flow rate of the samples was 0.3 ml/min as they were injected using a direct syringe pump. Mobile phase A and mobile phase B of the solvent system were configured. Formic acid 0.1 % was added to mobile phase A, which was water, and to mobile phase B, which was acetonitrile. A Peptide was eluted directly off the column into the LCQ system using a gradient of 5–95 %. The total run time was set at 30 min. The samples were fully scanned in positive mode with a mass range of 50–1000 *m/z*.

#### 3.5. Protein-protein interaction networks (PPINs)

The genes in the dataset were chosen based on a literature survey using the keyword "ERBB2 signalling pathway". The draft PPINs were constructed using the String v11.5 server with the highest confidence score of 0.9 (>90 % similarity) [27]. The network was constructed using direct interaction of each gene connected. The final network was validated and designed using the Cytoscape v3.10.0 [28]. Hub genes (highly interconnected genes/nodes that share high interaction with edges) were predicted using the CytoHubba module [29], and the network properties were predicted using the Network analyzer module [30] in the Cytoscape.

#### 3.6. Molecular docking

The molecular docking analysis has been carried out in Dassault Systems BIOVIA Discovery Studio v22.1.100, the licensed version. The three-dimensional structure of our target protein, HER2, was retrieved

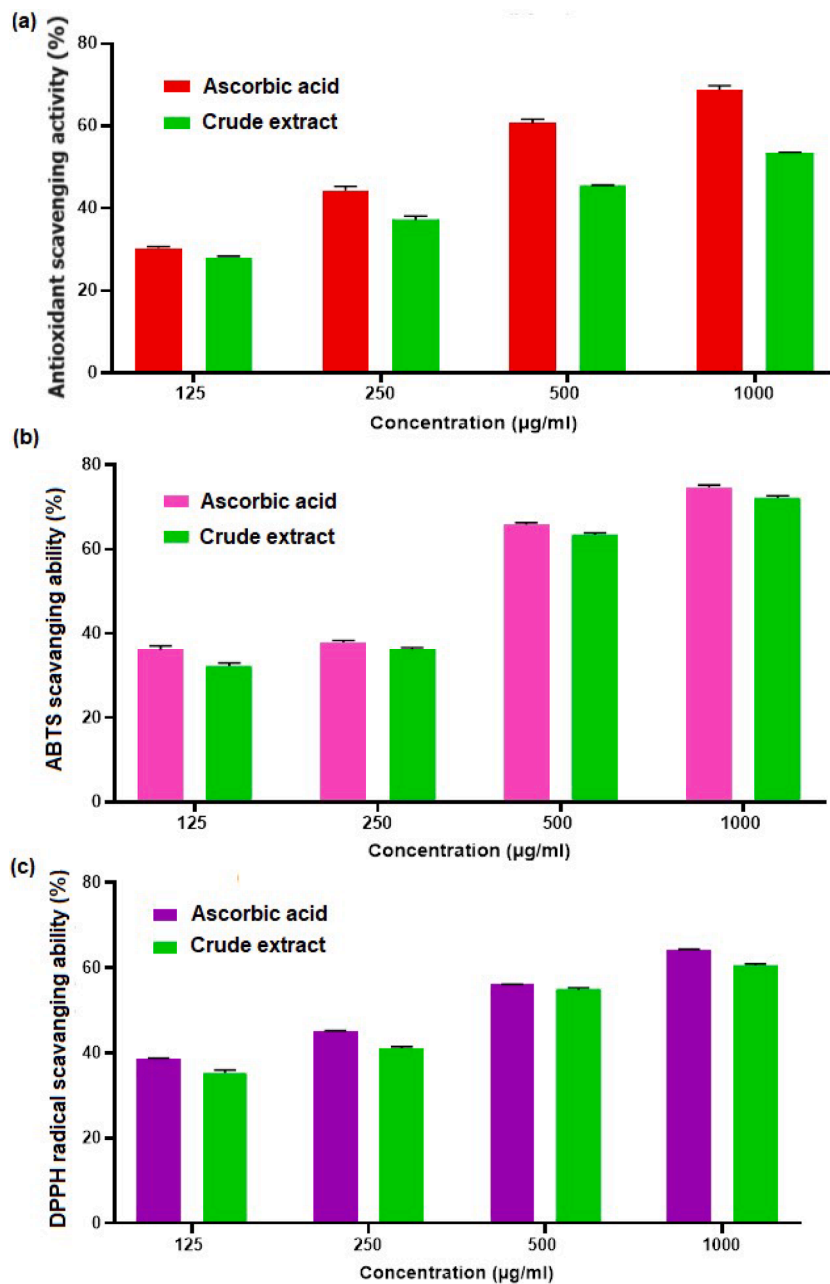
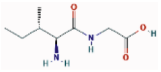
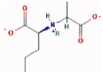
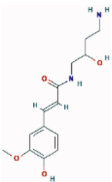
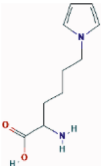


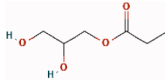
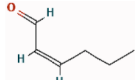
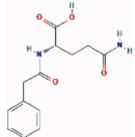
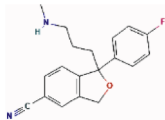
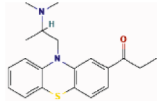
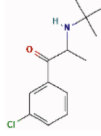
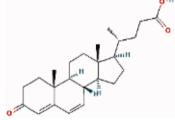
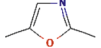
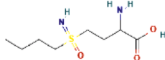
Fig. 3. DPPH free radical scavenging assay (a), ABTS scavenging activity (b), and total antioxidant free radical scavenging activity (c) of *B. cereus* crude methanolic extract and ascorbic acid.

**Table 2**  
HRLC-MS analysis of *B. cereus* methanolic extract (Positive).

S. No.	Retention time (RT)	Compound name	PubChem ID	Compound structure	Molecular formula	Molecular weight (g/mol)	Score	M/Z [+]	Hydrogen donor	Hydrogen acceptor	XLog	Lipdock Score value (SMY6)
1	1.344	Isoleucyl-Glycine	6,992,869		C <sub>8</sub> H <sub>16</sub> N <sub>2</sub> O <sub>3</sub>	188.1132	188.1135	211.1025	3	4	-2.3	88.559
2	1.465	(S)-2,3,4,5- Tetrahydropiperidine-2- carboxylate	45,266,761		C <sub>6</sub> H <sub>9</sub> NO <sub>2</sub>	127.0638	127.0638	150.053	0	3	0.5	62.748
3	1.465	Indole-3-methyl acetate	74,706		C <sub>11</sub> H <sub>11</sub> NO <sub>2</sub>	189.0795	189.0795	190.0867	1	2	1.7	88.1385
4	1.908	(2S)-2-([1-(R)- Carboxyethyl] amino)pentanoate	134,820,391		C <sub>8</sub> H <sub>15</sub> NO <sub>4</sub>	189.0993	189.0993	212.0886	1	4	-0.3	85.1256
5	2.462	(2R,3R,4R)-2-Amino-4- hydroxy-3- methylpentanoic acid	2,769,418		C <sub>6</sub> H <sub>13</sub> NO <sub>3</sub>	147.0891	189.0992	170.0782	3	4	-2.8	70.9589
6	2.653	N-Nitrosoproline	10,419,304		C <sub>5</sub> H <sub>8</sub> N <sub>2</sub> O <sub>3</sub>	144.0533	144.0533	167.0425	1	5	0.3	70.2523
7	2.844	L-2-Amino-3- methylenehexanoic acid	76,223,581		C <sub>7</sub> H <sub>13</sub> NO <sub>2</sub>	143.0941	143.0941	166.0834	2	3	-1	71.9301
8	2.885	Methyl N-methyl anthranilate	6826		C <sub>9</sub> H <sub>11</sub> NO <sub>2</sub>	165.0779	165.0779	188.0674	1	3	2.3	72.6886
9	3.069	Feruloyl-2-hydroxyputrescine	131,751,430		C <sub>14</sub> H <sub>20</sub> N <sub>2</sub> O <sub>4</sub>	280.1403	280.1403	303.129	4	5	0.1	104.295
10	3.65	Methpyrlylon	4162		C <sub>10</sub> H <sub>17</sub> NO <sub>2</sub>	183.125	183.125	206.1142	1	2	0.8	78.5001
11	3.773	L-alpha-Amino-1H-pyrrole-1- hexanoic acid	15,800,938		C <sub>10</sub> H <sub>16</sub> N <sub>2</sub> O <sub>2</sub>	196.1183	196.1183	197.1255	2	3	-1.9	96.1371

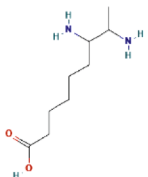
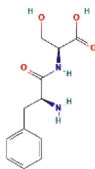
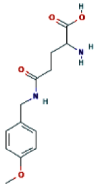
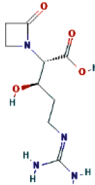
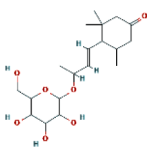
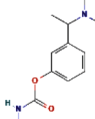
(continued on next page)

Table 2 (continued)

S. No.	Retention time (RT)	Compound name	PubChem ID	Compound structure	Molecular formula	Molecular weight (g/mol)	Score	M/Z [+]	Hydrogen donor	Hydrogen acceptor	XLog	Lipdock Score value (5MY6)
12	4.005	Glycerol 1-propanoate	117,335		C <sub>6</sub> H <sub>12</sub> O <sub>4</sub>	148.0734	148.0734	171.0625	2	4	-0.5	74.7084
13	4.172	(Z)-2-Hexenal	6,428,782		C <sub>6</sub> H <sub>10</sub> O	98.0733	98.0733	121.0625	0	1	1.5	51.382
14	4.315	Alpha-N-Phenylacetyl-L-glutamine	92,258		C <sub>13</sub> H <sub>16</sub> N <sub>2</sub> O <sub>4</sub>	264.1096	264.1096	287.0985	3	4	0	114.493
15	4.421	Demethylcitalopram	162,180		C <sub>19</sub> H <sub>19</sub> FN <sub>2</sub> O	310.1503	310.1503	333.14	1	4	2.8	111.245
16	4.487	Propiomazine	4940		C <sub>20</sub> H <sub>24</sub> N <sub>2</sub> OS	340.1606	340.1606	363.15	0	4	4.8	108.171
17	4.548	Bupropion	444		C <sub>13</sub> H <sub>18</sub> C <sub>1</sub> NO	239.1122	239.1122	240.1195	1	2	3.2	85.347
18	4.581	3-Oxochola-4,6-dien-24-oic Acid	5,283,992		C <sub>24</sub> H <sub>34</sub> O <sub>3</sub>	370.2523	370.2523	371.2596	1	3	5.2	68.9361
19	4.917	2,5-Dimethyloxazole	89,961		C <sub>5</sub> H <sub>7</sub> NO	97.053	97.053	120.0422	0	2	1.1	53.329
20	4.92	Buthionine sulfoximine	21,157		C <sub>8</sub> H <sub>18</sub> N <sub>2</sub> O <sub>3</sub> S	222.1026	222.1026	245.0917	3	5	-0.6	97.2777

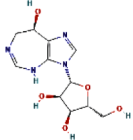
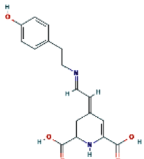
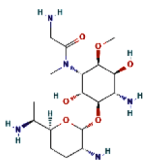
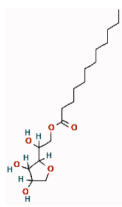
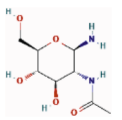
(continued on next page)

Table 2 (continued)

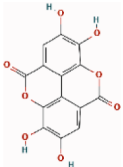
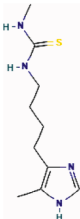
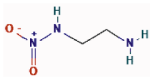
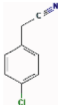
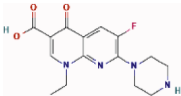
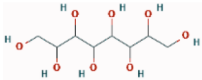
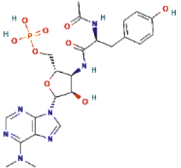
S. No.	Retention time (RT)	Compound name	PubChem ID	Compound structure	Molecular formula	Molecular weight (g/mol)	Score	M/Z [+]	Hydrogen donor	Hydrogen acceptor	XLog	Lipdock Score value (5MY6)
21	5.12	7,8-Diaminononanoate	652		C <sub>9</sub> H <sub>20</sub> N <sub>2</sub> O <sub>2</sub>	188.1516	188.1516	211.1408	3	4	-2.3	89.9719
22	5.381	Phenylalanyl-Serine	193,508		C <sub>12</sub> H <sub>16</sub> N <sub>2</sub> O <sub>4</sub>	252.1101	252.1101	275.099	4	5	-3.7	109.622
23	5.463	N5-(4-Methoxybenzyl)glutamine	131,751,461		C <sub>13</sub> H <sub>18</sub> N <sub>2</sub> O <sub>4</sub>	266.1249	266.1249	289.114	3	5	-2.3	115.589
24	5.82	Guanidinoproclavaminc acid	441,124		C <sub>9</sub> H <sub>16</sub> N <sub>4</sub> O <sub>4</sub>	244.1175	244.1175	245.1247	4	5	-2.7	119.712
25	5.966	9-Hydroxy-7-megastigmen-3-one glucoside	131,752,911		C <sub>19</sub> H <sub>32</sub> O <sub>7</sub>	372.2209	372.2209	373.2282	4	7	0.4	105.896
26	6.19	Miotine	46,093		C <sub>12</sub> H <sub>18</sub> N <sub>2</sub> O <sub>2</sub>	222.1357	222.1357	245.1247	1	3	1.6	84.7941

(continued on next page)

Table 2 (continued)

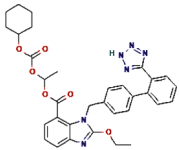
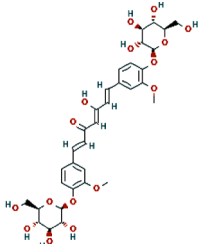
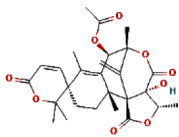
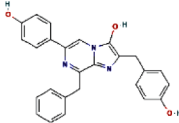
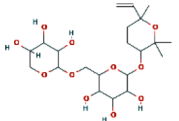
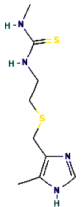
S. No.	Retention time (RT)	Compound name	PubChem ID	Compound structure	Molecular formula	Molecular weight (g/mol)	Score	M/Z [+]	Hydrogen donor	Hydrogen acceptor	XLog	Lipdock Score value (5MY6)
27	6.61	Coformycin	<a href="#">25,447</a>		C <sub>11</sub> H <sub>16</sub> N <sub>4</sub> O <sub>5</sub>	284.1117	284.1117	289.1136	5	7	-3.1	116.195
28	6.883	Miraxanthin-III	135,438,593		C <sub>17</sub> H <sub>18</sub> N <sub>2</sub> O <sub>5</sub>	330.1166	330.1166	331.1238	4	7	1.4	110.047
29	8.129	Fortimicin A	<a href="#">5,284,517</a>		C <sub>17</sub> H <sub>35</sub> N <sub>5</sub> O <sub>6</sub>	405.2598	405.2598	428.2489	6	10	-4.4	109.96
30	15.7	Sorbitan laurate	<a href="#">347,468</a>		C <sub>18</sub> H <sub>34</sub> O <sub>6</sub>	346.2357	346.2357	174.1252	3	6	3.7	110.258
31	15.783	N-Acetyl-b-glucosaminylamine	<a href="#">439,454</a>		C <sub>8</sub> H <sub>16</sub> N <sub>2</sub> O <sub>5</sub>	220.1065	220.1065	221.1137	5	6	-2	98.2361

**Table 3**  
 HRLC-MS analysis of *B. cereus* methanolic crude extract (Negative).

S. No.	Retention time (RT)	Compound name	PubChem ID	Compound structure	Molecular formula	Molecular weight (g/mol)	Score	M/Z [-]	Hydrogen donor	Hydrogen acceptor	XLog	Lipdock Score value
1	6.125	Ellagic acid	5,281,855		C <sub>14</sub> H <sub>6</sub> O <sub>8</sub>	302.0058	52.74	347.0031	4	8	1.1	113.021
2	0.963	4-Methylburimamide	3,084,972		C <sub>10</sub> H <sub>18</sub> N <sub>4</sub> S	226.1255	92.85	271.1236	3	2	0.8	99.4937
3	1.123	N-Nitroethylenediamine	194,053		C <sub>2</sub> H <sub>7</sub> N <sub>3</sub> O <sub>2</sub>	105.0534	75.81	150.0515	2	4	-0.4	54.2295
4	1.186	4-Chlorophenylacetonitrile	241,582		C <sub>8</sub> H <sub>6</sub> ClN	151.0213	35.46	196.0195	0	1	2.5	67.4204
5	2.95	Enoxacin	3229		C <sub>15</sub> H <sub>17</sub> FN <sub>4</sub> O <sub>3</sub>	320.1305	85.93	319.1233	2	8	-0.2	48.7013
6	3.446	D-erythro-d-galacto-octitol	219,890		C <sub>8</sub> H <sub>18</sub> O <sub>8</sub>	242.099	83.89	287.0972	8	8	-4.3	108
7	3.657	N-Acetyl-O-demethylpuromycin-5'-phosphate	46,173,767		C <sub>23</sub> H <sub>30</sub> N <sub>7</sub> O <sub>9</sub> P	579.1851	95.61	624.1831	6	13	-1.7	-

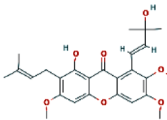
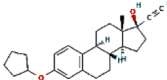
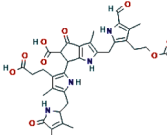
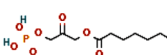
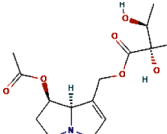
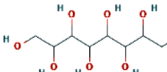
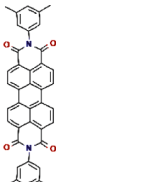
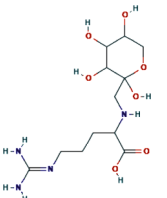
(continued on next page)

Table 3 (continued)

S. No.	Retention time (RT)	Compound name	PubChem ID	Compound structure	Molecular formula	Molecular weight (g/mol)	Score	M/Z [-]	Hydrogen donor	Hydrogen acceptor	XLog	Lipdock Score value
8	4.115	Candesartan cilextil	2540		C <sub>33</sub> H <sub>34</sub> N <sub>6</sub> O <sub>6</sub>	610.2505	74.89	655.249	1	10	7	-
9	4.333	Curcumin diglucoside	46,173,989		C <sub>33</sub> H <sub>40</sub> O <sub>16</sub>	692.232	94.85	691.2249	9	16	0.4	-
10	4.928	Austin	38,353,601		C <sub>27</sub> H <sub>32</sub> O <sub>9</sub>	500.2037	93.91	499.1967	1	9	1.4	-
11	4.688	Oplophorus luciferin	135,445,694		C <sub>26</sub> H <sub>21</sub> N <sub>3</sub> O <sub>3</sub>	423.1562	68.65	482.1698	3	5	5.5	-
12	4.799	Linalool 3,7-oxide beta-primeveroside	131,752,012		C <sub>21</sub> H <sub>36</sub> O <sub>11</sub>	464.2274	74.45	523.2434	6	11	-2.2	-
13	4.925	Metiamide	1,548,992		C <sub>9</sub> H <sub>16</sub> N <sub>4</sub> S <sub>2</sub>	244.0824	88.97	243.075	3	3	0.5	-

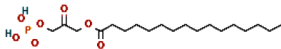
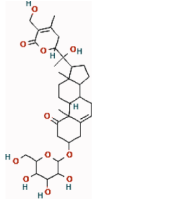
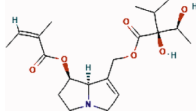
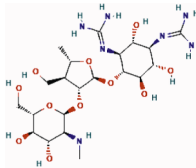
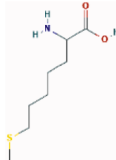
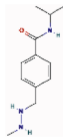
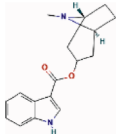
(continued on next page)

Table 3 (continued)

S. No.	Retention time (RT)	Compound name	PubChem ID	Compound structure	Molecular formula	Molecular weight (g/mol)	Score	M/Z [-]	Hydrogen donor	Hydrogen acceptor	XLog	Lipdock Score value
14	5.202	1-Hydroxy-3,6,7-trimethoxy-2-(3-methyl-2-butenyl)-8-(3-hydroxy-3-methyl-1E-butenyl)-xanthone	5,319,715		C <sub>26</sub> H <sub>30</sub> O <sub>7</sub>	454.1987	73.23	453.191	2	7	5.3	-
15	5.281	Quinestrol	9046		C <sub>25</sub> H <sub>32</sub> O <sub>2</sub>	364.2399	95.7	423.2538	1	2	5.3	-
16	5.338	Bn-NCC-1	131,752,318		C <sub>37</sub> H <sub>40</sub> N <sub>4</sub> O <sub>11</sub>	716.2773	51.71	715.2701	7	11	2.8	-
17	5.407	Palmitoylglycerone phosphate	167,650		C <sub>19</sub> H <sub>37</sub> O <sub>7</sub> P	408.2277	83.34	453.227	2	7	5.4	-
18	5.438	Uplandicine	156,778		C <sub>17</sub> H <sub>27</sub> NO <sub>7</sub>	357.1825	63.68	356.1757	3	8	-1.3	-
19	5.522	D-erythro-d-galacto-octitol	219,890		C <sub>8</sub> H <sub>18</sub> O <sub>8</sub>	242.0991	85.59	287.0974	8	8	-4.3	-
20	5.553	C.I. Pigment Red 149	62,555		C <sub>40</sub> H <sub>26</sub> N <sub>2</sub> O <sub>4</sub>	598.1892	58.22	597.187	0	4	8.3	-
21	5.647	N2-Fructopyranosylarginine	75,046,985		C <sub>12</sub> H <sub>24</sub> N <sub>4</sub> O <sub>7</sub>	336.1615	66.77	381.1599	8	9	-6.1	141.837

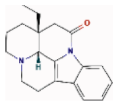
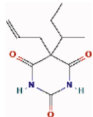
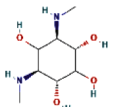
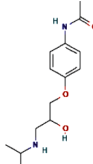
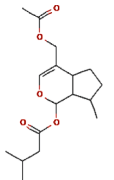
(continued on next page)

Table 3 (continued)

S. No.	Retention time (RT)	Compound name	PubChem ID	Compound structure	Molecular formula	Molecular weight (g/mol)	Score	M/Z [-]	Hydrogen donor	Hydrogen acceptor	XLog	Lipdock Score value
22	5.76	Palmitoylglycerone phosphate	167,650		C <sub>19</sub> H <sub>37</sub> O <sub>7</sub> P	408.2289	93.63	453.2274	2	7	5.4	149.487
23	6.423	(3b,20R,22R)-3,20,27-Trihydroxy-1-oxowitha-5,24-dienolide 3-glucoside	73,108,380		C <sub>34</sub> H <sub>50</sub> O <sub>11</sub>	634.3235	50.85	633.3165	6	11	1.4	-
24	7.105	Symlandine	5,281,753		C <sub>20</sub> H <sub>31</sub> NO <sub>6</sub>	381.2188	73.47	426.2171	2	7	1.3	94.2567
25	7.436	Dihydrodeoxystreptomycin	11,953,824		C <sub>21</sub> H <sub>41</sub> N <sub>7</sub> O <sub>11</sub>	567.2815	67.91	612.2798	12	14	-7.1	-
26	12.393	Trihomomethionine	22,266,650		C <sub>8</sub> H <sub>17</sub> NO <sub>2</sub> S	191.1017	52.98	236.0997	2	4	-1.1	82.2301
27	12.396	Procarbazine	4915		C <sub>12</sub> H <sub>19</sub> N <sub>3</sub> O	221.1496	33.47	220.1414	3	3	0.1	91.5776
28	12.458	Tropisetron	656,665		C <sub>17</sub> H <sub>20</sub> N <sub>2</sub> O <sub>2</sub>	284.1477	43.5	329.1459	1	3	3.8	113.071

(continued on next page)

Table 3 (continued)

S. No.	Retention time (RT)	Compound name	PubChem ID	Compound structure	Molecular formula	Molecular weight (g/mol)	Score	M/Z [-]	Hydrogen donor	Hydrogen acceptor	XLog	Lipdock Score value
29	12.698	Eburnamonine	92,112		C <sub>19</sub> H <sub>22</sub> N <sub>2</sub> O	294.1768	69.96	293.1695	0	2	3	104.738
30	17.9	Talbutal	8275		C <sub>13</sub> H <sub>20</sub> N <sub>2</sub> O <sub>3</sub>	252.1481	90.28	297.1466	2	3	1.4	90.8654
31	17.986	Actinamine	46,173,945		C <sub>8</sub> H <sub>18</sub> N <sub>2</sub> O <sub>4</sub>	206.1277	86.64	265.1418	6	6	-3.2	83.1021
32	19.828	Practolol	4883		C <sub>14</sub> H <sub>22</sub> N <sub>2</sub> O <sub>3</sub>	266.1636	92.59	311.162	3	4	0.8	94.1579
33	20.094	Valdiate	129,715,809		C <sub>17</sub> H <sub>26</sub> O <sub>5</sub>	310.1746	57.69	309.1674	0	5	3.1	98.8875

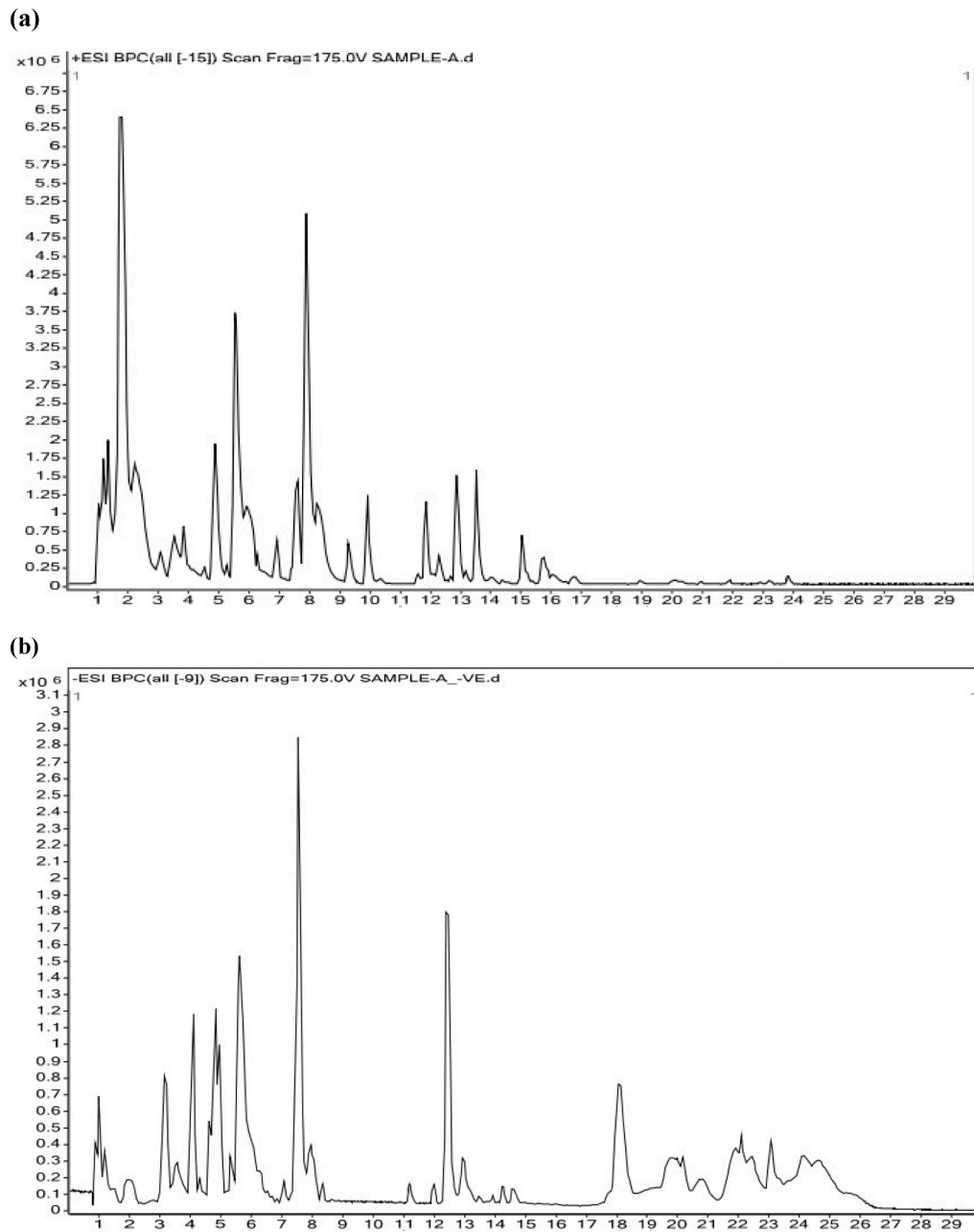
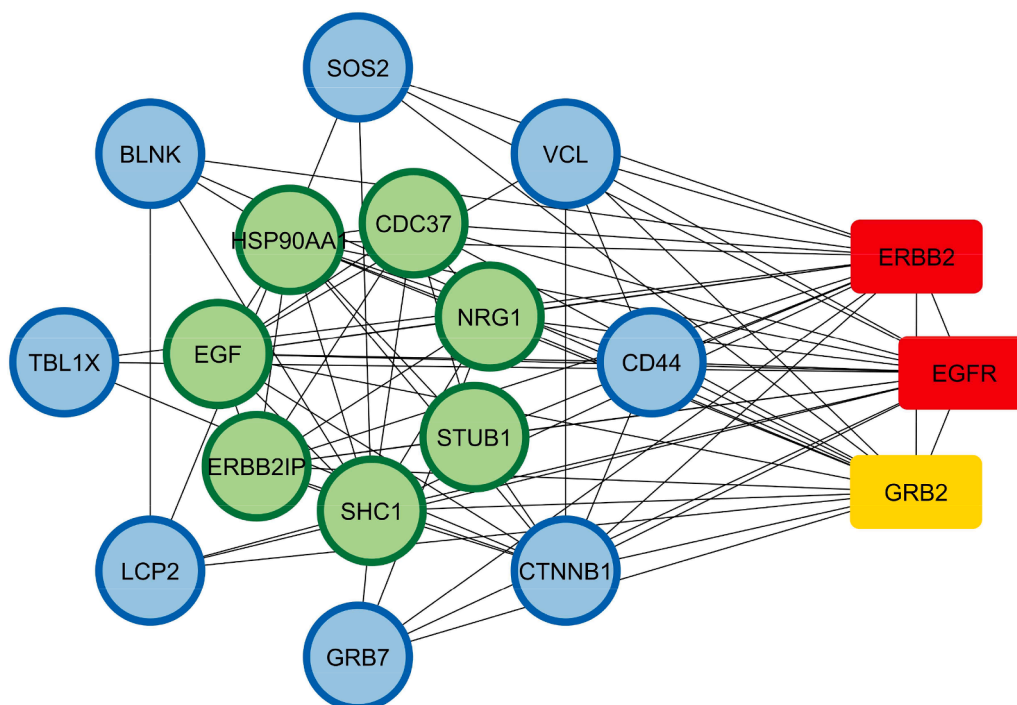


Fig. 4. HPLC-MS +Ve (a), and -Ve (b) chromatogram of methanolic *B. cereus* crude extract.



**Fig. 5.** Construction of PPINs of ERBB2 signaling pathway. **Note:** Green circle: represents the genes involved in the ERBB2 signaling pathway; blue circle: indicates genes involved in other pathways. The network consists of 18 nodes and 82 edges.

from the Protein Data Bank (PDB) using its PDB ID: 5MY6. Ligands were selected from *B. cereus* crude extract results based on the HRLC-MS. Protein preparation involves deleting water molecules, ligands, and ions, assigning bond orders, adding hydrogen atoms, and checking amino acid protonation states. Grid setup was used to find optimal binding positions, and docking was performed using the LibDock algorithm [31].

### 3.7. Cell line

For the cytotoxicity studies, MCF-7 (Human breast cancer cell line) was purchased from the National Centre for Cell Science (NCCS), Pune. It was cultured in liquid medium (DMEM) supplemented with 10 % Fetal Bovine Serum (FBS), 100 ug/ml penicillin and 100 µg/ml streptomycin, and maintained under an atmosphere of 5 % CO<sub>2</sub> at 37°C.

### 3.8. MTT assay

Cytotoxicity studies on MCF-7 human breast cancer cell lines were purchased from NCCS, Pune. The culture using DMEM, FBS, penicillin, streptomycin, and a 5 % CO<sub>2</sub> atmosphere at 37 °C. The bacterial crude extract was tested for *in vitro* cytotoxicity using the MCF-7 cell line using an MTT assay. Cultured MCF-7 cells were plated in 96-well tissue culture plates and treated with different concentrations of the crude sample. The cells were incubated at 37 °C for 24 h, then treated with MTT (20 µl) for 2–4 h until purple precipitates appeared. The medium and MTT were aspirated, and washed, and formazan crystals were dissolved [32]. The absorbance was measured at 570 nm, and the percentage cell viability and IC50 value were calculated using Graph Pad Prism 6.0 software.

## 4. Results

### 4.1. Identification of strain and phylogenetic tree construction

The bacteria were obtained from the marine soil sediment from the Velar estuary. The isolate was initially identified as a *Bacillus* species

because it was gram-positive, motile, rod-shaped, catalyze-positive, and aerobic bacterium (Fig. 1). The genomic DNA was amplified using 16S rRNA sequencing with 100 % similarity of the phylogenetic tree showed to *B. cereus* (Gen Bank Accession Number: OQ946984). The phylogenetic tree was further statistically validated by comparing pairwise genetic diversity and Tajima's neutrality test, as represented in Supplementary Tables S1 and S2. The sequence had a size of 1261 bp and was uploaded from the sequence we have constructed a phylogenetic tree using the Neighbor-Joining method to show related species [21]. In the bootstrap test, the percentage of replicate trees in which the associated taxa clustered together (1000 replicates) are shown above the branches [33]. This study included five nucleotide sequences. For each sequence pair, all ambiguous positions were removed (pairwise deletion option). There were a total of 1491 positions in the final dataset. The phylogenetic analysis was conducted using MEGA v11 [20].

### 4.2. FTIR analysis

FTIR analysis of bacterial crude extract was carried out to reveal the functional groups present in the *B. cereus* crude. FTIR spectrum showed the major peaks at 3790.4 cm<sup>-1</sup> are responsible for the O–H stretching of alcohol. The broad peak at 3338.18 cm<sup>-1</sup> is responsible for the N–H stretching of aliphatic primary amine. The straight peaks 2401.91 cm<sup>-1</sup> and 2348.87 cm<sup>-1</sup> are responsible for the O=C=O stretching of carbon dioxide. The remaining narrow peaks 2348.87, 2078.89, 1630.52, 1530.24, 1402.96, 1273.75, and 1222.65 cm<sup>-1</sup> revealed the presence of other compounds such as Isothiocyanate, cyclic alkene, nitro compound, sulfonyl compound, aromatic compound and vinyl ether in low amounts (Table 1 and Fig. 2).

## 5. Antioxidant activity

### 5.1. Total antioxidant scavenging activity

The total antioxidant scavenged by marine *B. cereus* extracts was found to increase with increasing concentration. Fig. 3a and

**Table 4**  
Interacting residues (Positive compounds).

S. No	Compound ID	Compound name	Hydrogen Bond	Hydrophobic
1	6,992,869	Isoleucyl-Glycine	A:HIS188, A:ARG189, A:PRO218, A:TYR240, A:ASP241, A:ARG244	A:ARG189, A:ARG244
2	45,266,761	(S)-2,3,4,5-Tetrahydropiperidine-2-carboxylate	A:PRO218, A:TYR240, A:ASP241	A:HIS188, A:LEU215, A:ARG244
3	74,706	Indole-3-methyl acetate	A:HIS188, A:ASP241	A:ARG189, A:PRO218, A:ARG244
4	134,820,391	(2S)-2-[[1-(R)-Carboxyethyl]amino]pentanoate	A:HIS188, A:ARG189, A:ASP241, A:ARG271	A:PRO218, A:TYR240
5	2,769,418	(2R,3R,4R)-2-Amino-4-hydroxy-3-methylpentanoic acid	A:GLY216, A:TYR240, A:ASP241, A:ARG244	A:PRO218, A:TYR240, A:ARG244
6	10,419,304	N-Nitrosoproline	A:HIS188, A:ARG189, A:GLY216	A:LEU215, A:PRO218, A:ARG244
7	76,223,581	L-2-Amino-3-methylenehexanoic acid	A:GLY216, A:PRO218	A:HIS188, A:PRO218, A:ARG244
8	6826	Methyl N-methyl anthranilate	A:ARG189, A:ASP241,	A:LEU215, A:TYR240, A:TYR245, A:PRO248
9	131,751,430	Feruloyl-2-hydroxyputrescine	A:GLN54, A:ASN259, A:PHE291, A:ALA293, A:SER294	-
10	4162	Methyprylon	A:ARG189, A:TYR240, A:ASP241	A:HIS188, A:LEU215, A:PRO218, A:ARG244, A:PRO248
11	15,800,938	L-alpha-Amino-1H-pyrrole-1- hexanoic acid	A:HIS188, A:ASP241, A:ARG271	A:PRO218, A:ARG244
12	117,335	Glycerol 1-propanoate	A:HIS188, A:ASP241, A:ARG271	A:PRO218, A:ARG244
13	6,428,782	(Z)-2-Hexenal	A:PRO218	A:HIS188, A:LEU215
14	92,258	Alpha-N-Phenylacetyl-l-glutamine	A:GLN57, A:ARG103, A:CYS255, A:ASN259, A:GLY292, A:SER294	-
15	162,180	Demethylcitalopram	A:ASN259, A:GLY292	A:VAL55, A:ALA293
16	4940	Propiomazine	A:ARG189, A:ASP217, A:TYR240, A:ASP241	A:ARG189, A:LEU191, A:PRO218, A:TYR240, A:ARG244, A:TYR245, A:PRO248
17	89,961	2,5-Dimethyloxazole	A:TYR240, A:ASP241	A:HIS188, A:PRO218, A:TYR240, A:ARG244, A:TYR245
18	21,157	Buthionine sulfoximine	A:GLN57, A:PHE291, A:GLY292	-

**Table 4 (continued)**

S. No	Compound ID	Compound name	Hydrogen Bond	Hydrophobic
19	652	7,8-Diaminononanoate	A:ARG189, A:GLY216, A:ASP241	A:HIS188, A:ARG189, A:PRO218, A:TYR240, A:ARG244
20	193,508	Phenylalanyl-Serine	A:ARG189, A:GLY216, A:PRO218, A:ASP241, A:ARG244	A:ARG189, A:ARG244
21	131,751,461	N5-(4- Methoxybenzyl) glutamine	A:LEU313, A:GLU321, A:TYR343, A:THR407	A:VAL341, A:PHE371
22	441,124	Guanidinoproclavaminic acid	A:LEU313, A:PRO316, A:GLN320, A:GLU321, A:TYR343	-
23	131,752,911	9-Hydroxy-7-megastigmen-3- one glucoside	A:GLY216, A:PRO218, A:TYR240, A:ASP241	A:ARG244, A:PRO248
24	46,093	Miotine	A:ARG189, A:GLY216, A:PRO248	A:ARG189, A:LEU191, A:PRO218, A:ARG244
25	25,447	Coformycin	A:GLU79, A:ARG103, A:ASN259, A:ALA293	-
26	135,438,593	Miraxanthin-III	A:ASP192, A:GLY216, A:PRO218, A:TYR240, A:ARG244	A:LEU191
27	5,284,517	Fortimicin A	A:HIS188, A:ARG189, A:GLY216, A:ASP217, A:PRO218, A:ASP241, A:ARG244	A:HIS188, A:ARG189, A:LEU215, A:ARG244
28	347,468	Sorbitan laurate	A:GLN24, A:ASN259, A:SER261, A:SER294, A:CYS295	A:VAL55, A:ALA293
29	439,454	N-Acetyl-b-glucosaminylamine	A:ARG189, A:ASP217, A:PRO218, A:PHE239, A:TYR240, A:ASP241	-

Supplementary Table S3 show the standard deviation of various concentrations of 125, 250,500, and 1000 µg/ml. The IC<sub>50</sub> values of total antioxidant radical scavenging activity of marine *B. cereus* extract for methanol was 28.33±1.01 and its IC<sub>50</sub> values were closer to standard ascorbic acid 31.23±1.02.

## 5.2. ABTS scavenging activity

The ABTS scavenged by the marine *B. cereus* crude extract was found to increase with increasing concentration. Fig. 3b and Supplementary Table S4 show the standard deviation of various concentrations of 125, 250,500, and 1000 µg/ml. The IC<sub>50</sub> values of ABTS radical scavenging activity of marine *B. cereus* extracts for methanol were 29.00±0.28 and its IC<sub>50</sub> values were closer to standard ascorbic acid 32.14±0.05.

**Table 5**  
Interacting residues (Negative compounds).

S. No	Compound ID	Compound name	Hydrogen Bond	Hydrophobic
1	5,281,855	Ellagic acid	A:ARG189, A:PRO218, A:ASP241, A:PRO248, A:ARG271	A:ARG189, A:LEU191, A:ARG244
2	3,084,972	4-Methylburimamide	A:GLN78, A:GLU79, A:ASN259, A:ALA293	A:VAL55
3	194,053	N-Nitroethylenediamine	A:ARG189, A:GLY216, A:ASP241, A:ARG271	–
4	3229	Enoxacin	A:ARG189	–
5	219,890	D-erythro-d-galactooctitol	A:HIS188, A:ARG189, A:GLY216, A:ASP241, A:ARG244, A:ARG271	–
6	1,548,992	Metiamide	A:GLN24, A:GLN57, A:GLU79, A:GLY292, A:ALA293	A:VAL25, A:VAL55, A:PHE291, A:ALA293
7	9046	Quinestrol	A:ASN259	A:VAL55
8	167,650	Palmitoylglycerone phosphate	A:CYS315, A:PRO316, A:HIS318	A:VAL314, A:CYS315, A:CYS338, A:VAL341, A:MET347, A:PHE371, A:ILE435
9	156,778	Uplandicine	A:GLN57, A:GLU79, A:ALA293, A:SER294	A:VAL55, A:ALA293
10	75,046,985	N2-Fructopyranosylarginine	A:LEU313, A:PRO316, A:LEU317, A:HIS318, A:ASN319, A:GLU321, A:TYR343, A:GLU348	A:VAL314, A:CYS315, A:PHE371
11	5,281,753	Symlandine	A:GLY216, A:ASP217, A:ARG244	A:HIS188, A:ARG189, A:LEU19, A:PRO248
12	22,266,650	Trihomomethionine	A:GLY216, A:ASP217, A:TYR240, A:ASP241	A:HIS188, A:ARG189, A:LEU191, A:ARG244
13	4915	Procarbazine	A:GLY216, A:ASP241	A:ARG189, A:LEU191, A:ARG244
14	656,665	Tropisetron	A:HIS188, A:ARG189, A:ASP192, A:GLY216, A:ASP241, A:ARG271	A:LEU191, A:ARG244
15	92,112	Eburnamonine	A:PRO248, A:ARG271	A:LEU191, A:LEU215, A:PRO218, A:ARG244
16	46,173,945	Actinamine	A:GLN24, A:GLU79, A:PHE291, A:ALA293, A:SER294	–

**Table 5 (continued)**

S. No	Compound ID	Compound name	Hydrogen Bond	Hydrophobic
17	4883	Practolol	A:GLN24, A:GLU79, A:ALA293	
18	129,715,809	Valdiate	A:SER294, A:GLN24, A:GLN54, A:GLN78	A:VAL55,

### 5.3. DPPH free radical scavenging assay

DPPH free radical scavenging activity is to find out the antiradical efficiency. DPPH has an absorption band at 517 nm, which disappears upon reduction by an antioxidant, and the electrons become paired off and bleaching of the colour. Stoichiometry depends on the number of electrons taken up from compounds. The IC<sub>50</sub> Value of marine *B. cereus* methanolic extract is 29.00±0.28 compared to standard ascorbic acid's IC<sub>50</sub> Value of 36.48±0.52. The scavenging activity values are depicted in Fig. 3c and Supplementary Table S5.

### 5.4. High resolution-liquid chromatography mass spectrometry (HR-LCMS)

The extracted *B. cereus* crude was analyzed using HR-LCMS to identify its chemical composition. The analysis identified 31 positive ion compounds with molecular weights ranging from 97 to 452 g/mol and 33 negative ion compounds with molecular weights ranging from 105 to 813 g/mol. The results were compared with known compounds identified are given (Tables 2, 3 and Fig. 4) [34].

### 5.5. Analysis of PPINs

The PPINs consist of 18 genes, of which 10 are directly involved in the ERBB2 signalling pathway. The network consists of 18 nodes and 82 edges, as represented in Supplementary Table S6, S7. Interestingly, we identified the top three hub genes that control an entire PPIN [35-41] in the biological and molecular mechanisms of the ERBB2 signalling pathway. Such genes are erbb-2, EGFR, and pro-epidermal growth factor (GRB2), as depicted in (Fig. 5; Supplementary Fig S1). The top-hit molecular function, biological process, and cellular components of the predicted network are represented in Supplementary Table S8-10. Based on the top-hit hub genes, molecular docking studies were performed.

### 5.6. Molecular docking

The three-dimensional structural features of target receptor HER2 (PDB ID: 5MY6) and its secondary structural elements are depicted in Supplementary Fig S2. All the 64 compounds from the HRLC-MS positive and negative ion results were docked against the protein. LibDock module of BIOVIA Discovery studio v22.1.100 licensed version was used to carry out the docking process. The LibDock score of each compound is shown in (Tables 4 and 5). From these results, four compounds had a very high LibDock score. Two positive ion compounds N5-(4-Methoxybenzyl) glutamine (LibDock score = 120.116) and Guanidinoproclavaminic acid (119.712) showed good binding affinity. Two negative ion compounds N2-Fructopyranosylarginine (LibDock score = 141.837) and Palmitoylglycerone phosphate (LibDock score = 149.489) have comparatively better binding affinity to the target protein than the negative ion compounds. Palmitoylglycerone phosphate had the highest LibDock score of 149.487. The molecular interaction of the compounds to the target protein was visualized using the BIOVIA Discovery studio v22.1.100 licensed version (Figs. 6 and 7). And residues involved in the docking of the compound are given in (Tables 4 and 5). The number of

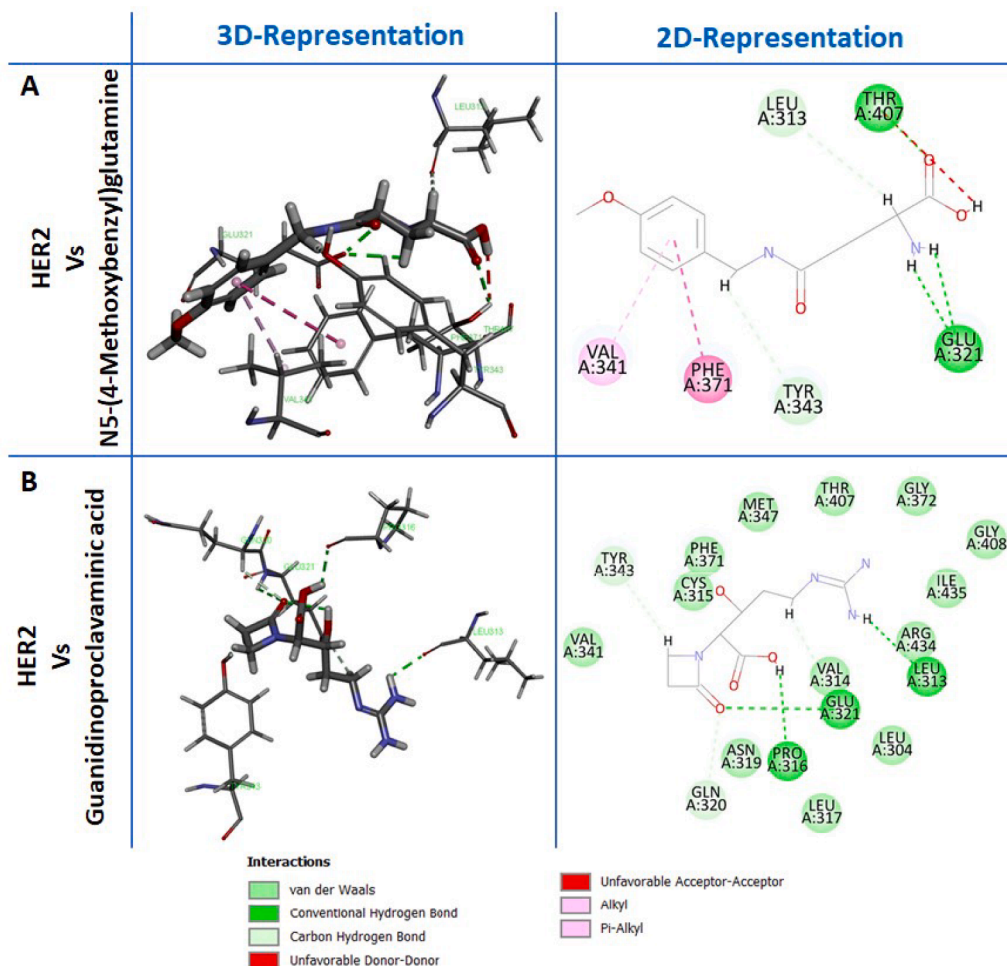


Fig. 6. Representation of 2D and 3D interaction view between N5-(4-Methoxybenzyl)glutamine (A), Guanidinoproclavaminic acid (B) against HER2 protein. Both compounds are positive ion compounds from the HRLC-MS analysis.

hydrogen and hydrophobic interactions of top hit docked complex of both positive and negative charged compounds was represented in Supplementary Fig S3 and S4. The compound interacted with low binding energy and a few interactions of the positive and negative docked complex were depicted in Supplementary Fig S5 and S6.

### 5.7. MTT assay

The effectiveness of *B. cereus* extract in inhibiting MCF-7 cell lines at different concentrations (1.56, 3.12, 6.25, 12.5, 25, 50, 100, 200 µg/ml) results are shown in Supplementary Table S11. The concentration-dependent effect of the bacteria test solution (crude extract) on the MCF-7 cell line is further supported by the cytotoxicity results shown in Fig. 8A-D. These results demonstrate that the tested species, marine *B. cereus* extract, were highly potent against cancer cells, with an IC<sub>50</sub> value of 3.12 µg/ml (Fig. 8E). To determine cytotoxicity, a marine *B. cereus* was tested on the standard Vero cell line. The results are shown in Supplementary Table S12. Cytotoxicity of Bacteria test solution at low, moderately toxic, and high concentrations is demonstrated, with a CC<sub>50</sub> value of 50 µg/ml. Marine *B. cereus* exhibits toxicity at high concentrations (Fig. 9). A high Therapeutic Index (TI) is crucial for a drug's safety profile. Understanding the preliminary TI early is crucial, as it indicates the likelihood of successful drug development. Calculating therapeutic values for isolated marine bacteria *B. cereus* with drug-like properties is essential (Table 6) [42].

## 6. Discussion

Cancer is still one of the most fatal diseases. Almost 60 % of anti-cancer drugs in use are of natural origin [43]. In various studies, it was reported that marine microorganisms have been a novel source for synthesizing diverse secondary metabolites with potent pharmacological activities [44-45]. They have certain advantages such as growing quickly, making the production of target substances easy to control, and being especially effective in large-scale production [45-46]. Breast cancer is a major threat to health among women worldwide. There is a need for a good biomarker to diagnose breast cancer in its early stage [47]. The amplification of HER2 has been reported in more than 15 – 30 % of invasive breast cancer cases [48]. *B. cereus*, a gram-positive rod-shaped bacteria reported to have various metabolites that have anti-cancer activity. A strain of *B. cereus* SVSK2 isolated from *Oreochromis mossambicus* had IC<sub>50</sub> of 300 µg/ml against an MCF-7 breast cancer cell line in an MTT assay [49]. And *B. cereus* from coastal wetland areas has high cellulolytic activity [50]. Based on this we have isolated *B. cereus* from the Velar estuary and investigated the properties of crude extract against the MCF-7 breast cancer cell line and *in silico* analysis against a particular breast cancer-associated receptor (HER2).

In this study we have identified *B. cereus* through morphological characterization, a rod-shaped bacterium with a violet color in gram staining showing that the organism is gram-positive, 16S rRNA gene sequencing was used to confirm the bacteria. The mass-cultivated culture was used to prepare the crude extract. By decreasing the free radicals and oxidative stress present in the body; antioxidants play a role in

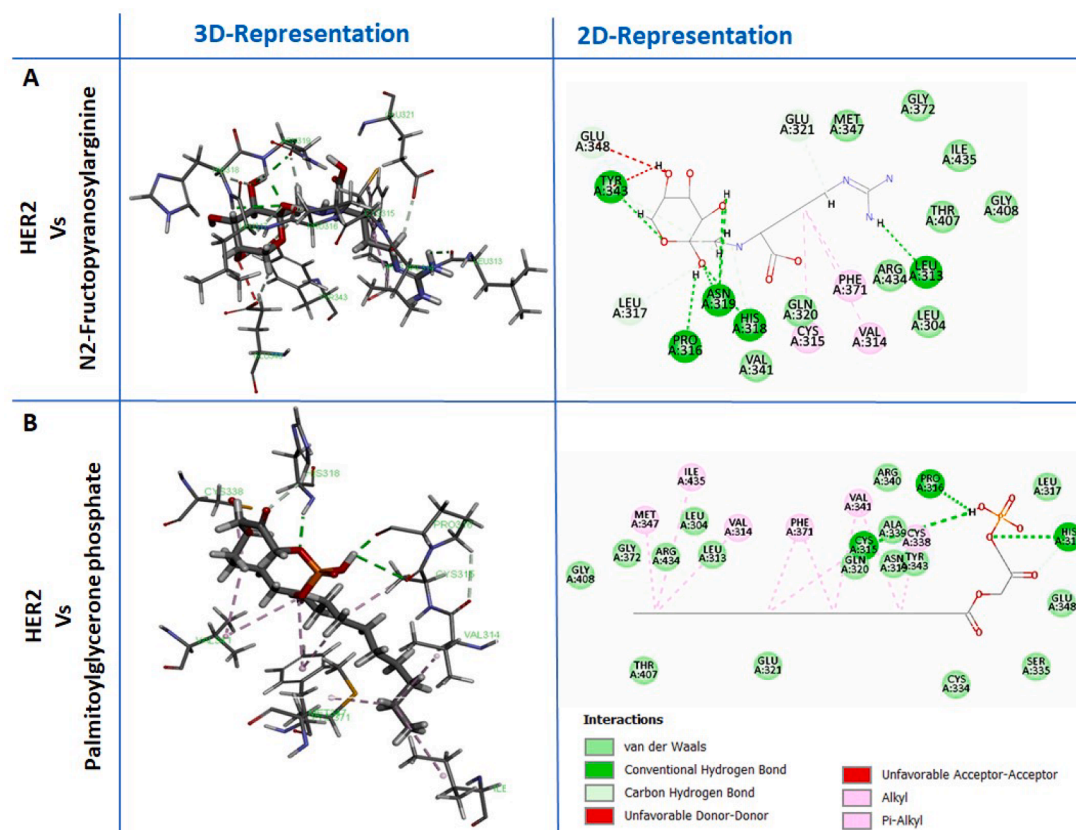


Fig. 7. Representation of 2D and 3D interaction view between N5-(4- N2-Fructopyranosylarginine (A), Palmitoylglycerone phosphate (B) against HER2 protein. Both compounds are negative ion compounds from the HRLC-MS analysis.

reducing the rate of abnormal cell division and decreasing mutagenesis [51]. Therefore, many antioxidant extracts show potent anticancer activity. To check for anticancer activity, we did some antioxidant assays with the *B. cereus* crude extract. The most widely employed methods to do free radical scavenging were DPPH, ABTS, and total antioxidant assay. The polarizability of the methanol solvent extraction was closer to standard ascorbic acid for all the above scavenging activity. The present study reported that methanol extract of marine *B. cereus* crude extract has potent antioxidant activity.

The presence of various compounds in the crude extract was identified through HRLC-MS. A total of 64 compounds were identified, 31 positive ion compounds and 33 negative ion compounds. The molecular docking analysis was done for all these 64 compounds against the HER2 protein. Of all the compounds 4 compounds had good interaction with the target proteins. N2- Fructopyranosylarginine had the LibDock score of 141.837 and Palmitoylglycerone phosphate had the LibDock score of 149.487 were the negative ion compounds. In positive ion compounds, Guanidinoproclavaminc acid had a LibDock score of 119.712, and N5-(4-Methoxybenzyl) glutamine had a LibDock score of 120.116. The compound N2-Fructopyranosylarginine have 8 hydrogen bond interactions with HER2 protein, the residues are A:LEU313, A:PRO316, A:LEU317, A:HIS318, A:ASN319, A:GLU321, A:TYR343, A:GLU348. Palmitoylglycerone phosphate has 3 hydrogen bond interactions with the target protein, the residues are A:CYS315, A:PRO316, A:HIS318. Guanidinoproclavaminc acid shares 5 hydrogen bonds and the residues are A:LEU313, A:PRO316, A:GLN320, A:GLU321, A:TYR343. N5-(4-Methoxybenzyl) glutamine also has 4 hydrogen bonds and the residues involved in that interaction are A:LEU313, A:GLU321, A:TYR343, A:THR407.

The *B. cereus* crude extract caused toxicity in cancer cell lines and also in normal cell lines. However, the toxicity effect was found more on cancer cells than on normal cells. The bacteria were able to inhibit the

proliferation of the cancer cell MCF-7 at low concentrations. However, they cause cytotoxicity to the normal Vero cells only at higher concentrations. In this regard, the therapeutic index is an important parameter as it includes anticancer activity and eventual toxicity to normal cells. This value is the ratio of the concentration of the extract at which 50 % of cytotoxicity occurred in a normal cell line to that of the test solution at which 50 % of cancer cell death occurred in cancer cell lines [52-53]. According to the American National Cancer Institute (NCI) recommendations, the limit of activity for crude extracts is 50 % inhibition (IC<sub>50</sub>) of proliferation was less than 30 g/ml following a 24-hour exposure duration [54]. In the present study, IC<sub>50</sub> values below this stringent point were noted with marine *B. cereus* against breast cancer. This species can be considered for the development of anticancer drugs.

Hence, in this study, marine *B. cereus* was tested for its anticancer activity. Human breast carcinoma cells (MCF-7), a normal cell line (VERO), a cell line, African Green Monkey kidney cell line were incubated separately with different doses of the marine *B. cereus* crude extracts. After 24 h, cell viability was determined by the MTT assay [32].

The anti-cancer activity of marine *B. cereus* was studied first against Breast cancer on the MCF-7 cell line, and it was found to be potent, as evident by the low concentration of less than 3.12 µg/ml at which 50 % of cancer cell death occurred on MCF-7. The IC<sub>50</sub> value was 3.12 µg/ml. The effect was concentration-dependent. The death rate of cancer cells increased with increasing concentrations of marine *B. cereus* test solutions.

It was found that a marine *B. cereus* extract is more toxic to cancer cells than a normal cell line. In this regard, the "therapeutic index" is a beneficial component to consider when choosing samples for new therapeutics. If a drug has a therapeutic index value of 16 or greater, it is considered worthy of further testing [42].

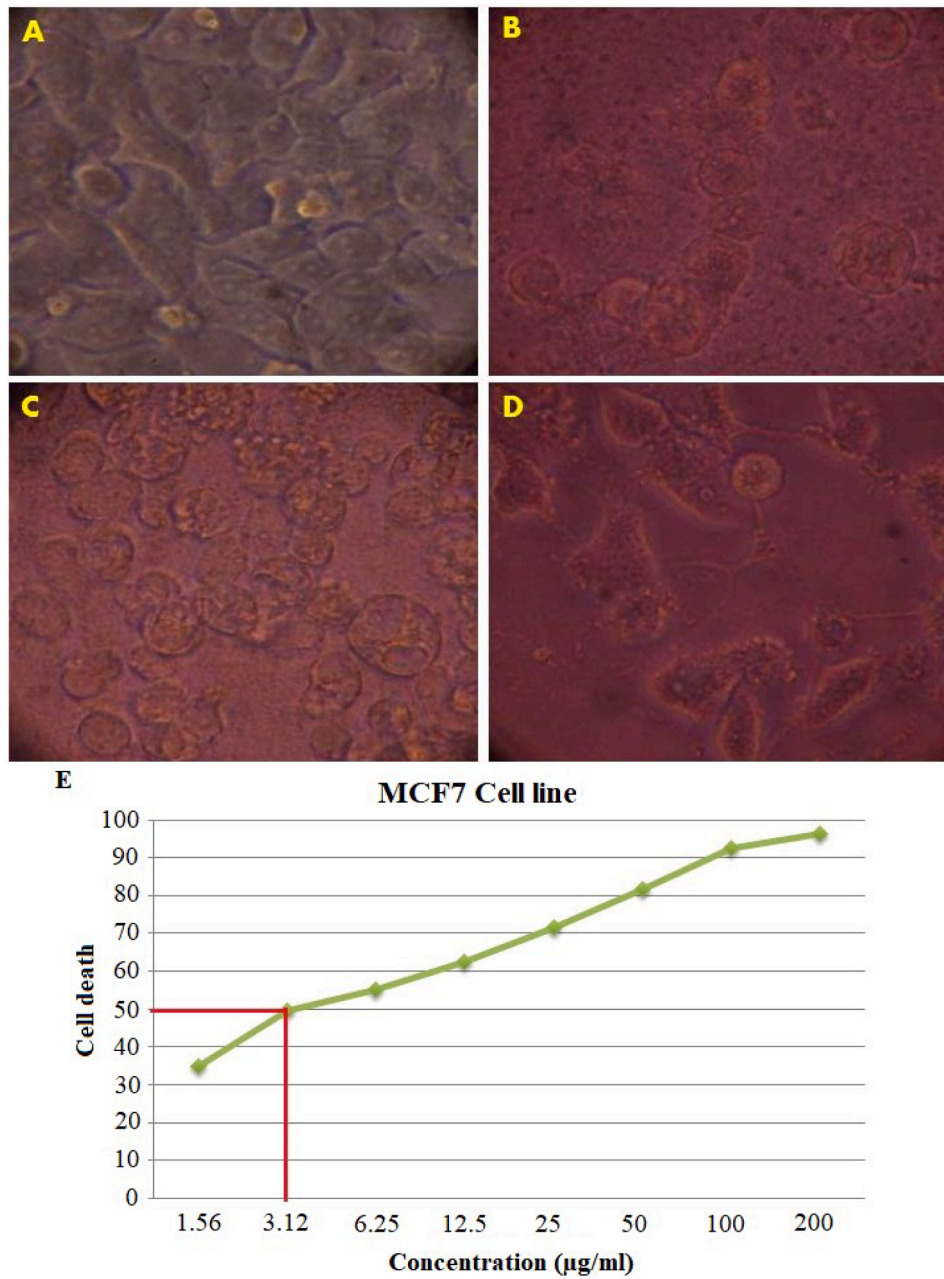


**Fig. 8.** Cytotoxic effects of the marine *B. cereus* extract on MCF7 Cell line: (A) Untreated MCF7 Cell Line, (B) High toxicity, (C) Medium toxicity, (D) Low toxicity concentrations, and (E) IC<sub>50</sub> value of marine *B. cereus* extract on MCF7 cell line cytotoxicity on the normal cell line.

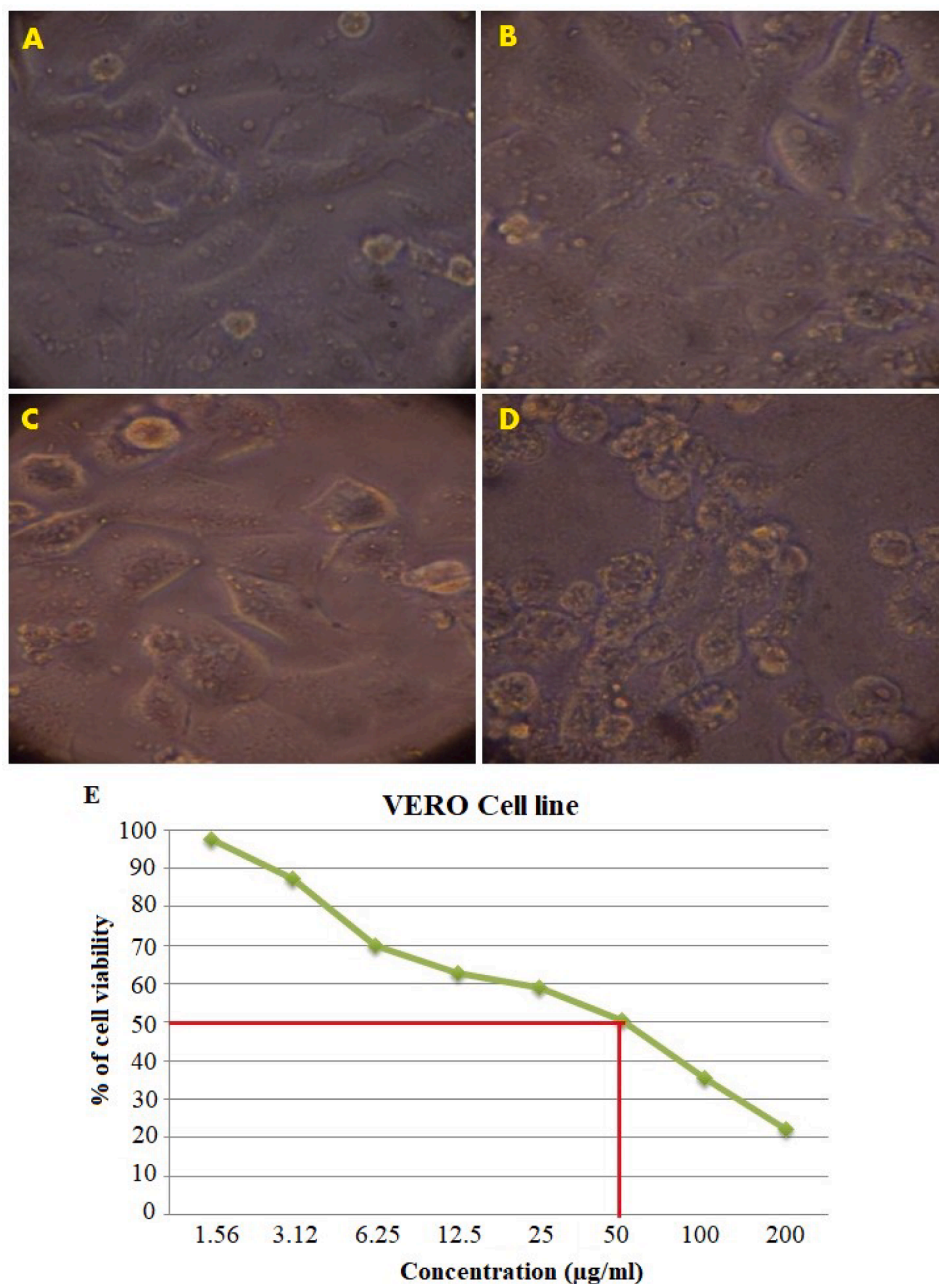


**Fig. 9.** Effect of marine *B. cereus* extract on the VERO cell line: (A) Untreated normal VERO cell line (B) Low concentration, (C) Medium concentration, (D) High concentration, and (E) Effect of marine *B. cereus* extracts at different concentrations on VERO cell line with CC<sub>50</sub> values.

**Table 6**

IC<sub>50</sub>, CC<sub>50</sub> and therapeutic values of marine *B. cereus* crude extract. **Note:** \*CC<sub>50</sub> the concentration at which 50 % cells survive in normal, IC<sub>50</sub> the concentration at which 50 % cell death occur treated.

Organism	MCF-7 Human Breast cancer cell line (IC <sub>50</sub> ) (µ/ml)	Normal VERO cell line (CC <sub>50</sub> ) (µg/ml)	Therapeutic Index (CC <sub>50</sub> / IC <sub>50</sub> ) MCF7
<i>B. cereus</i>	3.12	50	16

## 7. Conclusion

According to the results of the current study, bioactive metabolites isolated from *B. cereus* PSMS6 (OQ946984) exhibited *in vitro* anticancer activity against breast cancer (MCF-7) cells. Good LibDock scores were obtained against the targeted breast cancer protein HER2 in the *in-silico*

analysis of the bioactive compounds. Palmitoylglycerone phosphate demonstrated the best docking score for HER2 out of all the compounds. As a result, further research should concentrate on examining the molecular mechanisms and functions of the compound to gain a better understanding of breast cancer control and the development of anti-cancer drugs.

## Funding

This study was funded by the Tamil Nadu State Council for Higher Education (TANSCHÉ) through BDU-HECP-0068.

## Ethical approval

This article does not contain any studies with animals performed by any of the authors.

## CRedit authorship contribution statement

**Shalini TS:** Resources, Formal analysis. **Manivel G:** Supervision. **Krishna kumar G:** . **Prathiviraj Ragothaman:** Supervision. **Rajesh Kannan Velu:** Supervision. **Senthilraja P:** Writing – original draft, Visualization, Validation, Methodology, Investigation, Conceptualization.

## Declaration of competing interest

The author's declare that no conflict of interest in the present manuscript.

## Data availability

The data that has been used is confidential.

## Acknowledgments

None.

## Supplementary materials

Supplementary material associated with this article can be found, in the online version, at [doi:10.1016/j.btre.2024.e00842](https://doi.org/10.1016/j.btre.2024.e00842).

## References

- [1] A. Roheel, A. Khan, F. Anwar, Z. Akbar, M.F. Akhtar, M. Imran Khan, M. Farhan Sohail, R. Ahmad, Global epidemiology of breast cancer based on risk factors: a systematic review, *Front. Oncol.* 13 (2023) 1240098, <https://doi.org/10.3389/fonc.2023.1240098>.
- [2] L. Wilkinson, T. Gathani, Understanding breast cancer as a global health concern, *Br. J. Radiol.* 95 (1130) (2022) 20211033, <https://doi.org/10.1259/bjr.20211033>.
- [3] J. Wang, S.G. Wu, Breast cancer: an overview of current therapeutic strategies, challenge, and perspectives, *Breast Cancer (Dove Med Press)* 15 (2023) 721–730, <https://doi.org/10.2147/BCTT.S432526>.
- [4] H. Sung, J. Ferlay, R.L. Siegel, M. Laversanne, I. Soerjomataram, A. Jemal, F. Bray, Global cancer statistics 2020: GLOBOCAN estimates of incidence and mortality worldwide for 36 cancers in 185 countries, *CA Cancer J. Clin.* 71 (3) (2021) 209–249, <https://doi.org/10.3322/caac.21660>.
- [5] Cancer Research UK (2021) Breast Cancer Statistics. <https://www.cancerresearchuk.org/health-professional/cancer-statistics/statistics-by-cancer-type/breast-cancer>.
- [6] N. Howlader, S.F. Altekruse, C.I. Li, V.W. Chen, C.A. Clarke, L.A. Ries, K.A. Cronin, US incidence of breast cancer subtypes defined by joint hormone receptor and HER2 status, *J. Natl. Cancer Inst.* 106 (5) (2014) dju055, <https://doi.org/10.1093/jnci/dju055>.
- [7] US Food and Drug Administration (2019) <https://www.fda.gov/drugs>.
- [8] H.W. Ko, H.H. Lee, L. Huo, W. Xia, C.C. Yang, J.L. Hsu, L.Y. Li, C.C. Lai, L.C. Chan, C.C. Cheng, A.M. Labaff, H.W. Liao, S.O. Lim, C.W. Li, Y. Wei, L. Nie, H. Yamaguchi, M.C. Hung, GSK3 $\beta$  inactivation promotes the oncogenic functions of EZH2 and enhances methylation of H3K27 in human breast cancers, *Oncotarget* 7 (35) (2016) 57131–57144, <https://doi.org/10.18632/oncotarget.11008>.
- [9] J.L. Hsu, M.C. Hung, The role of HER2, EGFR, and other receptor tyrosine kinases in breast cancer, *Cancer Metastasis Rev.* 35 (4) (2016) 575–588, <https://doi.org/10.1007/s10555-016-9649-6>.
- [10] Z. Mitri, T. Constantine, R. O'Regan, The HER2 receptor in Breast cancer: pathophysiology, clinical use, and new advances in therapy, *Chemother. Res. Pract.* 2012 (2012) 743193, <https://doi.org/10.1155/2012/743193>.
- [11] J.A. Sparano, R.J. Gray, D.F. Makower, K.I. Pritchard, K.S. Albain, D.F. Hayes, C. E. Geyer, E.C. Dees, M.P. Goetz, J.A. Olson, T. Lively, S.S. Badve, T.J. Saphner, L. I. Wagner, T.J. Whelan, M.J. Ellis, S. Paik, W.C. Wood, P.M. Ravdin, M.M. Keane, H.L. Gomez Moreno, P.S. Reddy, T.F. Goggins, I.A. Mayer, A.M. Brufsky, D. L. Toppmeyer, V.G. Kaklamani, J.L. Berenberg, J. Abrams, G.W. Sledge, Adjuvant chemotherapy guided by a 21-gene expression assay in Breast cancer, *N. Engl. J. Med.* 379 (2) (2018) 111–121, <https://doi.org/10.1056/NEJMoa1804710>.
- [12] K. Kathiresan, A review of studies on Pichavaram mangrove, southeast India, *Hydrobiologia* 430 (2000) 185–205, <https://doi.org/10.1023/A:1004085417093>.
- [13] D.M. Hillis, M.T. Dixon, Ribosomal DNA: molecular evolution and phylogenetic inference, *Q. Rev. Biol.* 66 (4) (1991) 411–453, <https://doi.org/10.1086/417338>.
- [14] G. Manivel, D. Mathews Lurth Raj, R. Prathiviraj, P. Senthilraja, Distribution of phylogenetic proximity upon species-rich marine Ascomycetes with reference to Pichavaram mangrove soil sediment of southern India, *Gene Rep.* 21 (2020) 100878, <https://doi.org/10.1016/j.genrep.2020.100878>.
- [15] J.I. Carreto, M.O. Carignan, N.G. Montoya, A high-resolution reverse-phase liquid chromatography method for the analysis of mycosporine-like amino acids (MAAs) in marine organisms, *Mar. Biol.* 146 (2005) 237–252, <https://doi.org/10.1007/s00227-004-1447-y>.
- [16] L. Reyes-Escogido, M. Balam-Chi, I. Rodríguez-Buenfil, J. Valdés, L. Kameyama, F. Martínez-Pérez, Purification of bacterial genomic DNA in less than 20 min using chelex-100 microwave: examples from strains of lactic acid bacteria isolated from soil samples, *Antonie Van Leeuwenhoek* 98 (4) (2010) 465–474, <https://doi.org/10.1007/s10482-010-9462-0>.
- [17] T.C. Lorenz, Polymerase chain reaction: basic protocol plus troubleshooting and optimization strategies, *J. Vis. Exp.* (63) (2012) e3998, <https://doi.org/10.3791/3998>.
- [18] D.A. Benson, M. Cavanaugh, K. Clark, I. Karsch-Mizrachi, D.J. Lipman, J. Ostell, E. W. Sayers, GenBank, *Nucleic Acids Res* 41 (2013) D36–D42, <https://doi.org/10.1093/nar/gks1195>.
- [19] M. Johnson, I. Zaretskaya, Y. Raytselis, Y. Merezuk, S. McGinnis, T.L. Madden, NCBI BLAST: a better web interface, *Nucleic Acids Res.* 36 (2008) W5–W9, <https://doi.org/10.1093/nar/gkn201>.
- [20] S. Kumar, G. Stecher, M. Li, C. Knyaz, K. Tamura, X. MEGA, Molecular evolutionary genetics analysis across computing platforms, *Mol. Biol. Evol.* 35 (6) (2018) 1547–1549, <https://doi.org/10.1093/molbev/msy096>.
- [21] N. Saitou, M. Nei, The neighbor-joining method: a new method for reconstructing phylogenetic trees, *Mol. Biol. Evol.* 4 (4) (1987) 406–425, <https://doi.org/10.1093/oxfordjournals.molbev.a040454>.
- [22] F. Tajima, Statistical methods to test for nucleotide mutation hypothesis by DNA polymorphism, *Genetics* 123 (1989) 585–595.
- [23] J. Usmani, H. Kausar, S. Akbar, A. Sartaj, S.R. Mir, M.J. Hassan, M. Sharma, R. Ahmad, S. Rashid, M.N. Ansari, Molecular docking of bacterial protein modulators and pharmacotherapeutics of *Carica papaya* leaves as a promising therapy for sepsis: synchronising *in silico* and *in vitro* studies, *Molecules* 28 (2) (2023) 574, <https://doi.org/10.3390/molecules28020574>.
- [24] B. Halliwell, Free radicals, reactive oxygen species and human disease: a critical evaluation with special reference to atherosclerosis, *Br. J. Exp. Pathol.* 70 (6) (1989) 737–757.
- [25] R. Re, N. Pellegrini, A. Proteggente, A. Pannala, M. Yang, C. Rice-Evans, Antioxidant activity applying an improved ABTS radical cation decolorization assay, *Free Radic. Biol. Med.* 26 (9–10) (1999) 1231–1237, [https://doi.org/10.1016/S0891-5849\(98\)00315-3](https://doi.org/10.1016/S0891-5849(98)00315-3).
- [26] W. Brand-Williams, M.E. Cuvelier, C. Berset, Use of a free radical method to evaluate antioxidant activity, *LWT-Food Sci. Technol.* 28 (1) (1995) 25–30, [https://doi.org/10.1016/S0023-6438\(95\)80008-5](https://doi.org/10.1016/S0023-6438(95)80008-5).
- [27] D. Szklarczyk, A.L. Gable, D. Lyon, A. Jung, S. Wyder, J. Huerta-Cepas, M. Simonovic, N.T. Doncheva, J.H. Morris, P. Bork, L.J. Jensen, C.V. Mering, STRING v11: protein-protein association networks with increased coverage, supporting functional discovery in genome-wide experimental datasets, *Nucleic Acids Res.* 47 (D1) (2019) D607–D613, <https://doi.org/10.1093/nar/gky1131>.
- [28] P. Shannon, A. Markiel, O. Ozier, N.S. Baliga, J.T. Wang, D. Ramage, N. Amin, B. Schwikowski, T. Ideker, Cytoscape: a software environment for integrated models of biomolecular interaction networks, *Genome Res.* 13 (11) (2003) 2498–2504, <https://doi.org/10.1101/gr.123930>.
- [29] C.H. Chin, S.H. Chen, H.H. Wu, C.W. Ho, M.T. Ko, C.Y. Lin, cytoHubba: identifying hub objects and sub-networks from complex interactome, *BMC Syst. Biol.* 4 (2014) S11, <https://doi.org/10.1186/1752-0509-8-S4-S11>.
- [30] N.T. Doncheva, J.H. Morris, J. Gorodkin, L.J. Jensen, Cytoscape StringApp: network analysis and visualization of proteomics data, *J. Proteome Res.* 18 (2) (2019) 623–632, <https://doi.org/10.1021/acs.jproteome.8b00702>.
- [31] K. Kalidasan, L. Dufossé, G. Manivel, P. Senthilraja, K. Kathiresan, Antioxidant and anti-colorectal cancer properties in methanolic extract of Mangrove-derived *Schizochytrium* sp, *J. Mar. Sci. Eng.* 10 (3) (2022) 431, <https://doi.org/10.3390/jmse10030431>.
- [32] P. Senthilraja, K. Kathiresan, *In vitro* cytotoxicity MTT assay in Vero, HepG2 and MCF-7 cell lines study of Marine Yeast, *J. App. Pharm. Sci.* 5 (3) (2015) 080–084, <https://doi.org/10.7324/JAPS.2015.50313>.
- [33] J. Felsenstein, Confidence limits on phylogenies: an approach using the bootstrap, *Evolution (N Y)* 39 (4) (1985) 783–791, <https://doi.org/10.1111/j.1558-5646.1985.tb00420.x>.
- [34] E. Noumi, M. Snoussi, E.H. Anouar, M. Alreshidi, V.N. Veetil, S. Elkahoui, M. Adnan, M. Patel, A. Kadri, K. Aouadi, V. De Feo, R. Badraoui, HR-LCMS-based metabolite profiling, antioxidant, and anticancer properties of *Teucrium polium* L. methanolic extract: computational and *in vitro* study, *Antioxidants (Basel)* 9 (11) (2020) 1089, <https://doi.org/10.3390/antiox9111089>.
- [35] L. Dinesh Kumar, R. Prathiviraj, M. Selvakumar, R. Guna, E. Abbirami, T. Sivasudha, HRLC-ESI-MS based identification of active small molecules from *Cissus quadrangularis* and likelihood of their action towards the primary targets of osteoarthritis, *J. Mol. Struct.* 1199 (2020) 127048, <https://doi.org/10.1016/j.molstruc.2019.127048>.
- [36] T.R. Sivakumar, D. Surendhiran, K. Chen, P. Lv, A. Vinothkanna, R. Prathiviraj, S. Sethupathy, A.R. Sirajunnisa, Network pharmacology based analysis of *Astragalus propinquus* components for the treatment of rheumatoid arthritis and diabetes, *S. Afr. J. Bot.* 139 (2021) 92–105, <https://doi.org/10.1016/j.sajb.2021.01.034>.
- [37] G.S. Kiran, A. Sajayan, G. Priyadharshini, A. Balakrishnan, R. Prathiviraj, A. Sabu, J. Selvin, A novel anti-infective molecule nescantin identified from sponge associated bacteria *Nesterenkonia* sp. MSA31 against multidrug resistant *Pseudomonas aeruginosa*, *Microb. Pathog.* 157 (2021) 104923, <https://doi.org/10.1016/j.micpath.2021.104923>.

- [38] D.K. Lakshmanan, S. Murugesan, S. Rajendran, G. Ravichandran, A. Elangovan, K. Raju, R. Prathiviraj, R. Pandiyan, S. Thilagar, *Brassica juncea* (L.) Czern. leaves alleviate adjuvant-induced rheumatoid arthritis in rats via modulating the finest disease targets - IL2RA, IL18 and VEGFA, *J. Biomol. Struct. Dyn.* 40 (18) (2022) 8155–8168, <https://doi.org/10.1080/07391102.2021.1907226>.
- [39] A. Vinothkanna, R. Prathiviraj, T.R. Sivakumar, Y. Ma, S. Sekar, GC-MS and network pharmacology analysis of the ayurvedic fermented medicine, Chandanasava, against chronic kidney and cardiovascular diseases, *Appl. Biochem. Biotechnol.* 195 (5) (2023) 2803–2828, <https://doi.org/10.1007/s12010-022-04242-7>.
- [40] R. Prathiviraj, K.K. Adithya, R. Rajeev, R. Taslim Khan, S. Hassan, J. Selvin, G. Seghal Kiran, Alleviation of migraine through gut microbiota-brain axis and dietary interventions: coupling epigenetic network information with critical literary survey, *Trends Food Sci. Technol.* 141 (2023) 104174, <https://doi.org/10.1016/j.tifs.2023.104174>.
- [41] K. Barathikannan, R. Chelliah, A. Vinothkanna, R. Prathiviraj, A. Tyagi, S. Vijayalakshmi, M.J. Lim, A.Q. Jia, D.H. Oh, Untargeted metabolomics-based network pharmacology reveals fermented brown rice towards anti-obesity efficacy, *NPJ Sci. Food* 8 (1) (2024) 20, <https://doi.org/10.1038/s41538-024-00258-x>.
- [42] P.Y. Muller, M.N. Milton, The determination and interpretation of the therapeutic index in drug development, *Nat. Rev. Drug Discov.* 11 (10) (2012) 751–761, <https://doi.org/10.1038/nrd3801>.
- [43] A. Rayan, J. Raiyn, M. Falah, Nature is the best source of anticancer drugs: indexing natural products for their anticancer bioactivity, *PLoS ONE* 12 (11) (2017) e0187925, <https://doi.org/10.1371/journal.pone.0187925>.
- [44] L.E. Petersen, M.Y. Kellermann, P.J. Schupp, Secondary metabolites of marine microbes: from natural products chemistry to chemical ecology, in: S. Jungblut, V. Liebich, M. Bode-Dalby (Eds.), *YOUMARES 9 - The oceans: Our research, Our Future*, Springer, Cham, 2020, [https://doi.org/10.1007/978-3-030-20389-4\\_8](https://doi.org/10.1007/978-3-030-20389-4_8).
- [45] A. Karthikeyan, A. Joseph, B.G. Nair, Promising bioactive compounds from the marine environment and their potential effects on various diseases, *J. Genet. Eng. Biotechnol.* 20 (1) (2022) 14, <https://doi.org/10.1186/s43141-021-00290-4>.
- [46] R. Montaser, H. Luesch, Marine natural products: a new wave of drugs? *Future Med. Chem.* 3 (12) (2011) 1475–1489, <https://doi.org/10.4155/fmc.11.118>.
- [47] F.M. Alkabban, T. Ferguson, *Breast Cancer. StatPearls* [Internet], StatPearls Publishing, Treasure Island (FL), 2022.
- [48] N. Iqbal, N. Iqbal, Human epidermal growth factor receptor 2 (HER2) in cancers: overexpression and therapeutic implications, *Mol. Biol. Int.* 2014 (2014) 852748, <https://doi.org/10.1155/2014/852748>.
- [49] V. Seerangaraj, K. Suruli, U. Vijayakumar, B. Meganathan, V. Seerangara, S. Selvam, V. Rajendran, J. Selvaraj, Isolation and characterization of bioactive compounds for *Bacillus cereus* and *Bacillus subtilis* from *Oreochromis mossambicus* and *Labeo rohita*, *Int. J. Pharm. Sci. Rev. Res.* 43 (2) (2017) 71–77.
- [50] A. Chantarasiri, Aquatic *Bacillus cereus* JD0404 isolated from the muddy sediments of mangrove swamps in Thailand and characterization of its cellulolytic activity, *Egypt. J. Aquat. Res.* 41 (3) (2015) 257–264, <https://doi.org/10.1016/j.ejar.2015.08.003>.
- [51] B. Al-Dabbagh, I.A. Elhaty, A. Al Hrouf, R. Al Sakkaf, R. El-Awady, S.S. Ashraf, A. Amin, Antioxidant and anticancer activities of *Trigonella foenum-graecum*, *Cassia acutifolia* and *Rhazya stricta*, *BMC Complement. Altern. Med.* 18 (1) (2018) 240, <https://doi.org/10.1186/s12906-018-2285-7>.
- [52] G.J. Peters, H.H. Backus, S. Freemantle, B. van Triest, G. Codacci-Pisanelli, C.L. van der Wilt, K. Smid, J. Lunec, A.H. Calvert, S. Marsh, H.L. McLeod, E. Bloemena, S. Meijer, G. Jansen, C.J. van Groeningen, H.M. Pinedo, Induction of thymidylate synthase as a 5-fluorouracil resistance mechanism, *Biochim. Biophys. Acta.* 1587 (2–3) (2002) 194–205, [https://doi.org/10.1016/s0925-4439\(02\)00082-0](https://doi.org/10.1016/s0925-4439(02)00082-0).
- [53] J. Bré, A.L. Dickson, O.J. Read, Y. Zhang, F.G. McKissock, P. Mullen, P. Tang, G. M. Zickuhr, C.M. Czekster, D.J. Harrison, The novel anti-cancer fluoropyrimidine NUC-3373 is a potent inhibitor of thymidylate synthase and an effective DNA-damaging agent, *Cancer Chemother. Pharmacol.* 91 (5) (2023) 401–412, <https://doi.org/10.1007/s00280-023-04528-5>.
- [54] M. Suffness, J.M. Pezzuto, Assays related to cancer drug discovery. In: K. Hostettmann (ed). *Methods in Plant Biochemistry: Assays for Bioactivity*, Academic Press, London, 6 (1990) 71–133.